

This article appeared in a journal published by Elsevier. The attached copy is furnished to the author for internal non-commercial research and education use, including for instruction at the authors institution and sharing with colleagues.

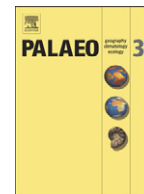
Other uses, including reproduction and distribution, or selling or licensing copies, or posting to personal, institutional or third party websites are prohibited.

In most cases authors are permitted to post their version of the article (e.g. in Word or Tex form) to their personal website or institutional repository. Authors requiring further information regarding Elsevier's archiving and manuscript policies are encouraged to visit:

<http://www.elsevier.com/authorsrights>

Contents lists available at [SciVerse ScienceDirect](http://www.sciencedirect.com)

Palaeogeography, Palaeoclimatology, Palaeoecology

journal homepage: www.elsevier.com/locate/palaeo

Paleoenvironmental changes during the Middle Eocene Climatic Optimum (MECO) and its aftermath: The benthic foraminiferal record from the Alano section (NE Italy)

F. Boscolo Galazzo ^{a,*}, L. Giusberti ^a, V. Luciani ^b, E. Thomas ^{c,d,e}

^a Department of Geosciences, University of Padova, Via G. Gradenigo 6, Italy

^b Department of Physics and Earth Sciences, University of Ferrara, Via G. Saragat 1, Italy

^c Department of Geology and Geophysics, Yale University, New Haven, CT, USA

^d Department of Earth and Environmental Sciences, Wesleyan University, Middletown, CT, USA

^e School of Earth Sciences, University of Bristol, UK

ARTICLE INFO

Article history:

Received 25 May 2012

Received in revised form 4 March 2013

Accepted 24 March 2013

Available online 3 April 2013

Keywords:

Middle Eocene Climatic Optimum (MECO)

Benthic foraminifera

Marine productivity

Sea floor oxygenation

Central-western Tethys

Alano section

Italy

ABSTRACT

The Middle Eocene Climatic Optimum (MECO) was one of the most severe, short-term global climate perturbations of the Cenozoic that occurred at ca. 40 Ma and was characterized by a gradual 4–6 °C temperature increase of intermediate and deep-waters. We investigated the response to the MECO of the deep-sea ecosystem in the central-western Tethys, through a quantitative study of bathyal benthic foraminiferal assemblages in the expanded and continuous Alano section (northeastern Italy), for which data on stratigraphy, lithology, isotope and trace element geochemistry, and calcareous microplankton were available. During the gradual warming of MECO (lasting between 350 and 650 kyr) marine export productivity increased, causing a significant but transient restructuring of benthic foraminiferal faunas, which changed gradually from assemblages typical for oligo-mesotrophic sea floor conditions to assemblages indicative of more eutrophic conditions. Just after the peak MECO conditions, which lasted less than 100 kyr, a prolonged phase of environmental instability (~500 kyr) occurred, marked by even more highly increased export productivity leading to bottom-water oxygen depletion, as reflected in deposition of organic-rich sediments and multiple peaks of bi-triserial opportunistic benthic foraminiferal taxa, including buliminids, bolivinids and uvigerinids. The high productivity may have been caused by a strong influx of nutrient-bearing fresh water into the basin, due to the increased vigour of the hydrological cycle during the warm period, and this increased fresh-water influx might have been a factor in enhancing water column stratification, thus exacerbating the hypoxic conditions, which persisted about 400–500 kyr. After deposition of the organic-rich layers the environmental perturbation ended, and benthic foraminiferal assemblages recovered while conditions became very similar to what they were before the MECO. The environmental disturbance during and directly after the MECO thus strongly but transiently affected benthic foraminiferal assemblages in the central western Tethys.

© 2013 Elsevier B.V. All rights reserved.

1. Introduction

The Eocene was a crucial time in the Earth's Cenozoic climate evolution. The highest temperatures of the Cenozoic were reached in the early Eocene (Early Eocene Climatic Optimum or EECO, ~52–50 Ma), followed by long-term high-latitude and deep-water cooling, which continued through the middle and late Eocene (Zachos et al., 2001; Katz et al., 2008; Zachos et al., 2008; Bijl et al., 2010). During this cooling, the Earth has been said to be in the so-called “doubthouse” climate state, between the “greenhouse” conditions of the early Paleogene

(high temperatures and pCO₂ levels, no polar ice sheets reaching sea level; e.g., Pagani et al., 2005) and the “icehouse” regime, starting with the development of the Antarctic continental ice sheet in the earliest Oligocene (Miller et al., 1987; Zachos et al., 1996; Coxall et al., 2005; Miller et al., 2005; Lear et al., 2008). During the “doubthouse” conditions, small, ephemeral ice sheets may have been present on the Antarctic continent but did not reach sea level (Miller et al., 2005), while sea ice may have been present in the Arctic Ocean (Stickley et al., 2009).

The long transition to globally cooler climates was interrupted by transient warming events (e.g., Tripathi et al., 2005; Sexton et al., 2006; Edgar et al., 2007), the most prolonged and intense of which was the Middle Eocene Climatic Optimum (MECO; Bohaty and Zachos, 2003). The MECO interrupted the cooling trend of the middle-late Eocene at ~40.6–40.0 Ma (Bohaty et al., 2009). It was first identified in Southern Ocean sediment cores as a transient oxygen

* Corresponding author. Tel.: +39 0498279183; fax: +39 0498279134.

E-mail addresses: flavia.boscologalazzo@studenti.unipd.it (F. Boscolo Galazzo), luca.giusberti@unipd.it (L. Giusberti), lcv@unife.it (V. Luciani), ellen.thomas@yale.edu (E. Thomas).

isotopic excursion (~–1.0‰) (Bohaty and Zachos, 2003), then recognized and more precisely dated in isotopic records from different areas (Jovane et al., 2007; Bohaty et al., 2009).

The ~500–750 kyr MECO warming (as expressed in an oxygen isotope excursion, OIE) started gradually, followed by a short interval of maximum warming (<100 kyr; Bohaty et al., 2009; Edgar et al., 2010), then ended by rapid cooling to pre-event values, within 200 kyr (Bohaty et al., 2009). The $\delta^{18}\text{O}$ records indicate warming of ~4–6 °C of both surface and deep waters (Bohaty et al., 2009; Edgar et al., 2010). High-latitude sea-surface temperatures (SSTs) ranged as high as 28 °C during the peak of the event, as estimated from organic-biomarker proxies (Bijl et al., 2010). The 500–750 kyr long duration and the pattern of gradual warming followed by rapid cooling clearly differentiate the MECO from late Paleocene through early Eocene hyperthermals with durations of 40–170 kyr, and either symmetrical beginning and ending, or a rapid start with gradual recovery (Bohaty et al., 2009; Bowen and Zachos, 2010; Galeotti et al., 2010; Stap et al., 2010; Zachos et al., 2010).

The MECO also differs from these earlier hyperthermals because the latter characteristically show global negative carbon isotope excursions (CIE) coeval with the OIE indicating warming, the CIEs reflecting the emission of isotopically negative carbon compounds in the ocean–atmosphere (e.g., review in Lunt et al., 2011; McInerney and Wing, 2011). These hyperthermals thus are considered equivalent to global warming caused by anthropogenic carbon emissions, and are associated with deep-sea ocean acidification and carbonate dissolution (e.g., Zachos et al., 2005; Hoensch et al., 2012). In contrast, MECO carbon isotope records vary geographically and bathymetrically (e.g., Spofforth et al., 2010). Oceanic $\delta^{13}\text{C}$ records show considerable geographic variability, but have generally rising $\delta^{13}\text{C}$ values across MECO, with a brief, ~0.5‰ negative CIE during peak warming of MECO only, clearly postdating the early, gradual warming (Bohaty et al., 2009, fig. 4; Edgar et al., 2010).

Despite the lack of CIE coeval with the warming, i.e., evidence for large-scale emission of isotopically negative carbon compounds into the atmosphere, there is evidence for 2–3 times increased atmospheric CO_2 levels during MECO from organic biochemical proxies (Bijl et al., 2010). Evidence for ocean acidification is less clear, because no records of direct dissolution proxies have been published (e.g., clay layers, fractionation of foraminifera). The occurrence of low carbon accumulation rates during MECO at sites located at depths of more than about 3400 m in the South Atlantic and Indian Oceans, however, has been interpreted as reflecting acidification (Bohaty et al., 2009). In conclusion, the MECO warming thus has been considered due to increased atmospheric CO_2 levels as the result of emission of carbon compounds with not markedly negative isotopic composition, so that their emission would not be seen in a significant, negative CIE, e.g., CO_2 from decarbonation during metamorphism and/or volcanic activity (Bohaty et al., 2009).

Despite the fact that extreme warming events of the Paleogene deeply affected the biota, as e.g., the Paleocene–Eocene Thermal Maximum (PETM; e.g., Sluijs et al., 2007; McInerney and Wing, 2011), surprisingly few studies have been devoted to the biotic response to the MECO in ocean drilling sections, an exception being the study on siliceous plankton in the southern Indian Ocean (Witkowski et al., 2012). At these locations there was a significant increase in biosiliceous sedimentation associated with the MECO, as well as rapid assemblage changes in autotrophic and heterotrophic siliceous microfossil groups.

MECO has been recognized in Italian sections, representing deposition in the western Tethys Ocean, having been first recognized in the Contessa section (paleodepth 800–1000 m), for which litho- and biomagnetostratigraphic data were presented (Jovane et al., 2007). Bulk $\delta^{13}\text{C}$ values show a positive excursion of ~0.6 per mille during MECO, but $\delta^{18}\text{O}$ records are diagenetically strongly overprinted so there is no direct evidence for warming. More detailed records have become available on the expanded and continuous Alano di Piave section (north-eastern Italy), for which Spofforth et al. (2010) presented

lithological, trace metal geochemistry and stable isotope records. A detailed magnetobiostratigraphy of the full Alano di Piave section was published by Agnini et al. (2011), showing the longer-term time frame, and placing the MECO in higher Chron C18r and Chron C18n2n, within nannofossil zones CP14a and NP16. The paleodepth during MECO was middle bathyal (600–1000 m; Agnini et al., 2011). A detailed record of MECO planktonic foraminiferal biotic events in this section was presented by Luciani et al. (2010), and of calcareous nannofossil events by Toffanin et al. (2011), making this section the only one for which detailed biotic records of carbonate microfossil assemblages across the MECO have been described.

At Alano, features of the MECO as described from deep-sea sections (Bohaty et al., 2009) have been recognized, including the gradual onset of the MECO at ~40.5 Ma, with progressively lower oxygen isotopic values (upper part of magnetochron C18r), minimum $\delta^{18}\text{O}$ values representing peak warming at the base of C18n.2n (~40.13 Ma), and recovery of the $\delta^{18}\text{O}$ values to background values over less than 100 kyr (Spofforth et al., 2010). The Alano section shows a negative $\delta^{13}\text{C}$ excursion in bulk carbonate associated with the MECO gradual warming as shown in bulk $\delta^{18}\text{O}$ values. Directly above the sediment interval reflecting MECO peak warming, however, the Alano section differs from the deep sea sections, because there are two intervals with a high organic carbon content and a trace element signature indicative of low oxygen conditions (Spofforth et al., 2010). This interval has a positive $\delta^{13}\text{C}$ excursion in bulk carbonate, now correlated with the excursion in the Contessa section (Jovane et al., 2007). This positive CIE has been interpreted as an indication of enhanced marine productivity, which may have led to sequestration of CO_2 from the ocean–atmosphere system in carbon-rich sediments, at least on a regional scale (Spofforth et al., 2010).

Both planktonic foraminifera and calcareous nannofossils reflect major environmental disturbance during MECO (Luciani et al., 2010; Toffanin et al., 2011), but no detailed records are available on the benthic foraminifera, thus the sea floor environment. We therefore performed a quantitative study of the MECO benthic foraminiferal assemblages in order to characterize changes in the benthic ecosystem of a bathyal environment during a yet poorly understood climatic perturbation. Through the integration of benthic foraminiferal data with published planktonic biotic and geochemical data we aim to better constrain the environmental and ecological changes across the Middle Eocene Climatic Optimum from a central-western Tethys perspective.

2. Setting, lithology and biostratigraphy

A continuous and expanded middle to upper Eocene section of grey marls crops out along the Calcino torrent riverbed, close to the village of Alano di Piave (Venetian Prealps, northeastern Italy). The section consists of 120–130 m monotonous grey marls, with intercalated silty–sandy tuff layers and biocalcarenitic–calciruditic beds (Agnini et al., 2011), and spans the upper part of Chron C18r (~41.5 Ma) to the base of Chron C16r (~36.5 Ma). The marls were deposited at middle-bathyal paleodepth (Agnini et al., 2011) in the Belluno Basin, a paleogeographic unit which originated in the Jurassic as the result of regional rifting and subsequent collapse of Triassic shallow-water carbonate platforms (e.g., Winterer and Bosellini, 1981). Hemipelagic sedimentation persisted until the late Eocene in the south-western sector of the Belluno Basin (Cita, 1975; Trevisani, 1997), which was surrounded by the structural high of the Lessini Shelf to the west (Bosellini, 1989) and of the Friuli Platform to the east (Fig. 1), with the section about 100–150 km away from the nearest land during sediment deposition. Because of its excellent exposure, abundant calcareous plankton and stratigraphical completeness, the Alano section has been proposed as candidate for the Global Stratotype Section and Point (GSSP) of the Priabonian (Agnini et al., 2011).

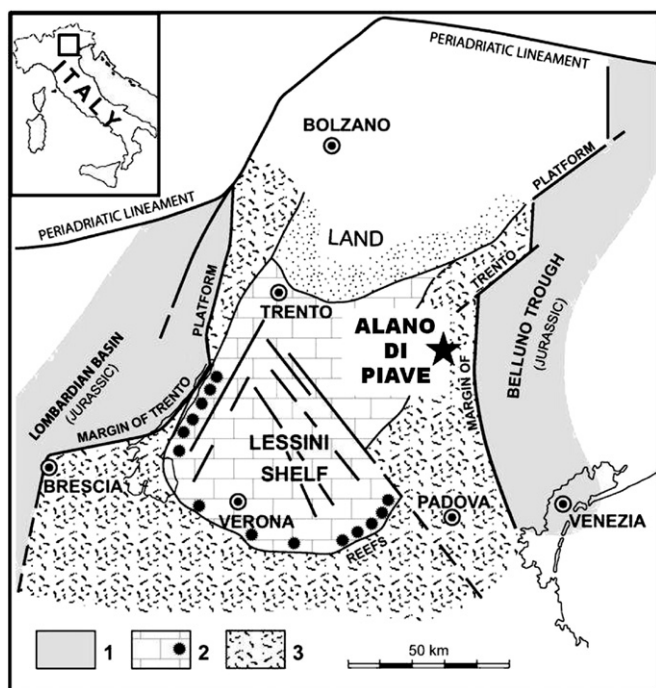


Fig. 1. Main paleogeographic elements of the Southern Alps during the Paleogene (modified from Bosellini, 1989) and location of Alano section (star). Legend: 1) deep-water mudstones of the Jurassic basins; 2) Paleogene lagoon and shelf edge reefs; 3) Palaeogene pelagic claystones and marlstones.

This study focuses on the interval from 10 to 32 m above the base of the section, which falls in planktonic foraminiferal Zones E10–11, E12 and lower E13 (Berggren and Pearson, 2005) or P12 to lower P14 (Berggren et al., 1995), and calcareous nannofossil Zone NP16 (Martini, 1971) or CP 14a (Okada and Bukry, 1980), as described by Agnini et al. (2011). Between 17 and 25 m, the dominant marly facies is interrupted by a ~8 m thick sapropel-like interval, which consists of laminated, dark grey to-black, marlstones (Fig. 2). This interval is characterized by an increase of the total organic carbon content (TOC) as well as sulphur, and pyrite is common (Spofforth et al., 2010). Redox-sensitive trace element patterns indicate low-oxygen conditions. The sapropel-like level can be subdivided into two sub-units (ORG1 and ORG2; Spofforth et al., 2010), separated by a 2 m-thick, lighter coloured and organic poor, marly interval (~19 to ~21 m, Fig. 2).

In this section, the base of the gradual $\delta^{18}\text{O}$ negative excursion is at 13 m (~40.5 Ma), and the OIE reaches its peak (ca. -3.4%) between 16.90 and 17 m, just below the base of the lower sapropel-like subunit (ORG1). The $\delta^{13}\text{C}$ and CaCO_3 records mirror this pattern and, after a gradual decrease, reach minimum values of -0.2% (from 1%) and 20% (from 60%) respectively at ~16.90–17 m (Fig. 2). This brief interval, with minimum isotopic and carbonate values, has been interpreted as the peak of MECO.

The interval overlying the MECO isotopic excursion (between ca. 17 and 25 m; Fig. 2) includes the ORG1 and ORG2 horizons, and is defined as “post-MECO interval” (Luciani et al., 2010). Agnini et al. (2011) estimate that the duration of the MECO and the post-MECO interval together was about 800–900 kyr (see also Spofforth et al., 2010). In the post-MECO interval, $\delta^{18}\text{O}$ values rapidly increase, and by 25 m recover to pre-event values. Within the 17–25 m interval, the $\delta^{13}\text{C}$ record is complex and strongly correlated with lithological changes. Two positive excursions between 19 and 21 m are similar in magnitude (1.25%), and coincide with the elevated TOC levels in intervals ORG1 and ORG2 (up to 3%; Fig. 2), interrupted by a negative excursion to near pre-event values.

3. Materials and methods

3.1. Benthic foraminifera

Benthic foraminifera were extracted from the marlstones using our standard method, disaggregation with 10–30% concentration hydrogen peroxide, for 1–2 h, followed by washing over ≥ 63 and ≥ 450 μm sieves. When necessary, samples were additionally soaked in a surface-tension-active solution. Finally, some samples were gently sonicated in order to break up clumps of residue. Quantitative analysis of benthic foraminiferal assemblages was performed on 39 samples from the 22 m interval described above. Sample spacing is 40 cm over the interval corresponding to the $\delta^{18}\text{O}$ isotopic shift, and on average 80 and 100 cm below and above this interval. Quantitative study was based on representative splits of residues (using a micro-splitter Jones, Geneq Inc.), counting at least 280 specimens larger than 63 μm and <450 μm (Appendix A). The use of the small-size fraction is time-consuming and presents difficulties in taxonomic determination, but we preferred to avoid the loss of small taxa, which are important for paleoecological investigations (e.g., Thomas 1985; Schroeder et al., 1987; Boltovskoy et al., 1991; Thomas et al., 1995; Giusberti et al., 2009). More than 250 taxa were identified at specific or higher taxonomic level, mainly following Hagn (1956), Braga et al. (1975), Grünig and Herb (1980), Grünig (1984, 1985), Parisi and Coccioni (1988), Barbieri (1990), and Ortiz and Thomas (2006). Additional analyses were carried out on the ≥ 450 μm size fraction: specimens were identified and counted (Appendix B), and absolute and relative abundance was calculated. The most representative taxa were photographed using SEM (scanning electron microscope).

Relative abundance of the common taxa (>5%) was calculated (Figs. 3, 4), together with faunal indices commonly used in paleoenvironmental reconstruction: the Fisher α diversity index and the dominance (using the PAST package; Hammer et al., 2001), the absolute abundance (N/g: number of benthic foraminifera per gram of sediment), the infaunal–epifaunal ratio (mainly following Corliss, 1985; Jones and Charnock, 1985; Corliss and Chen, 1988; Kaminski and Gradstein, 2005), the relative abundance of bi-triserial taxa and the agglutinated-calcareous ratio. Bi-triserial taxa percentage was calculated as the sum of all the buliminids minus the relative abundance of *Bolivinooides crenulata*, since this species shows a very different trend in abundance than the other bi-triserial taxa (Figs. 2, 3). The comparison of changes in relative and absolute abundance allows evaluating of the importance of the “fixed sum” problem (Thomas et al., 1995).

Relative abundance and faunal indices were calculated excluding fragments of astrophidids, an informal group in which we lumped all fragments of tubular, branching forms such as *Rhabdammina* and *Rhizammina*. In the residues it is difficult to estimate the number of individuals of these taxa, because only small fragments of these fragile forms (which are usually rare) were found. In order to avoid the loss of their signal completely, the absolute abundance of astrophidid fragments was calculated. Infaunal/epifaunal ratio and bi-triserial taxa percentages were calculated excluding “small trochospiral hyaline” and indeterminate trochospiral hyaline (ITH) specimens (see Appendix C). STH and ITH were excluded in calculating relative abundance.

Deep-water benthic foraminiferal communities are dominantly influenced by two environmental parameters: the food supply (quantity, quality and periodicity of the flux of food particles to the sea floor) and the oxygenation of bottom and/or pore waters (e.g., Lutze and Coulbourn, 1984; Corliss and Chen, 1988; Herguera and Berger, 1991; Loubere, 1991; Sen Gupta and Machain-Castillo, 1993; Alve, 1995; Jorissen et al., 1995; Loubere, 1996; Bernhard et al., 1997; Bernhard and Sen Gupta, 1999; Loubere and Fariduddin, 1999a,b; Morigi et al., 2001; Gooday, 2003; Jorissen et al., 2007). Benthic foraminifera are able to adapt to a wide spectrum of trophic conditions (e.g., Murray, 2006, 2013), but many taxa have an optimum range

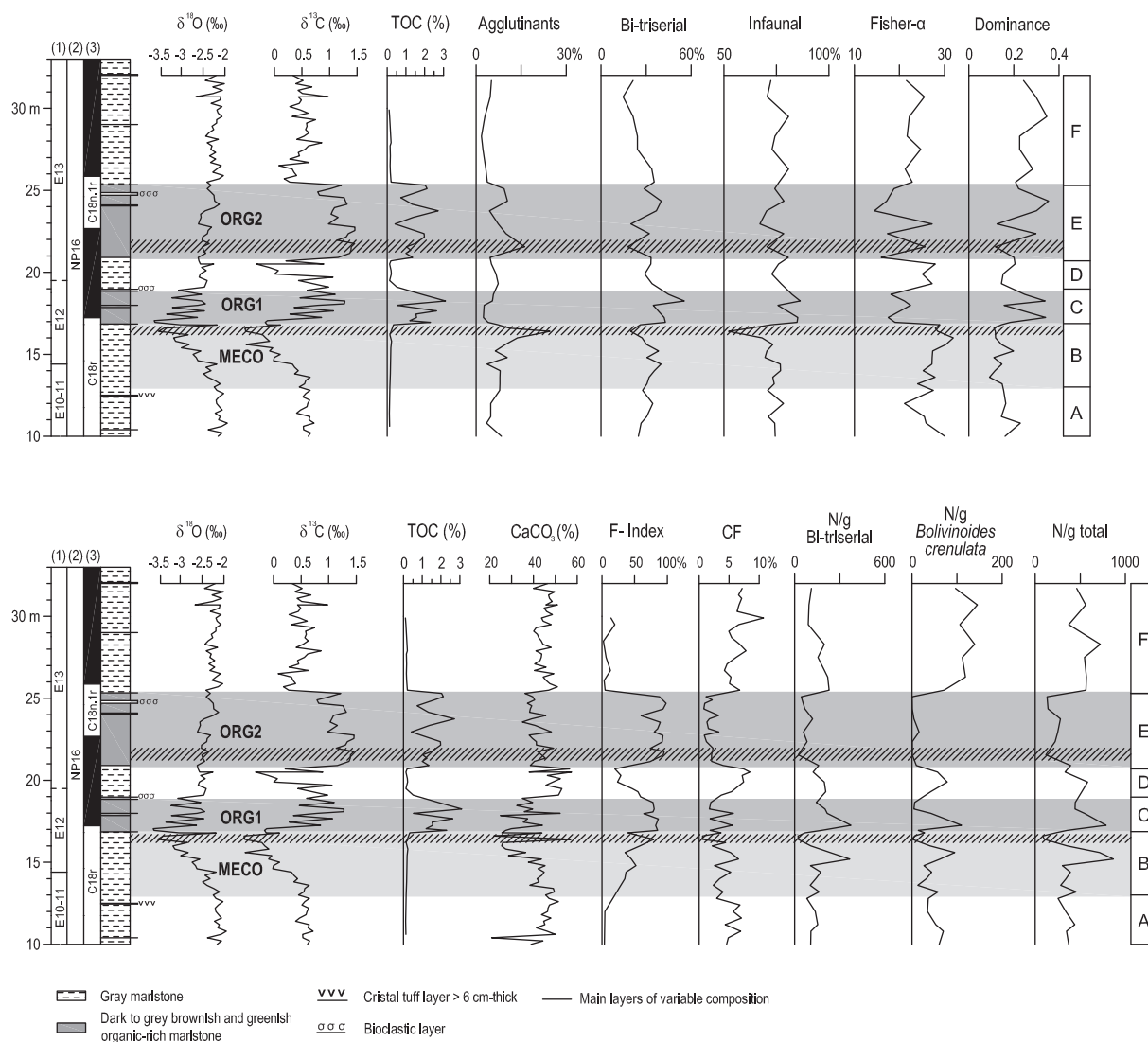


Fig. 2. Faunal and geochemical variations across the MECO at Alano plotted against bio-magnetostratigraphy, lithology and recognized benthic foraminiferal assemblages (A to F). Agglutinants = agglutinated to agglutinated and calcareous-hyaline ratio; Bi-triserial = cumulative relative abundance of the buliminids minus *Bolivinooides crenulata*; Infaunal = infaunal to infaunal and epifaunal ratio; Fisher- α and Dominance diversity indices; N/g Bi-triserial = number of bi-triserial benthic foraminifera per gram minus *Bolivinooides crenulata* in the $\geq 63 < 450 \mu\text{m}$ size fraction; N/g *Bolivinooides crenulata* = number of *Bolivinooides crenulata* per gram in the $\geq 63 < 450 \mu\text{m}$ size fraction and N/g total = number of benthic foraminifera per gram (faunal density) in the $\geq 63 < 450 \mu\text{m}$ size fraction. Stable isotopes ($\delta^{18}\text{O}$ and $\delta^{13}\text{C}$), total organic carbon (TOC%) and $\text{CaCO}_3\%$ are from Spofforth et al. (2010). Fragmentation index and coarse fraction (F-index and CF) are from Luciani et al. (2010). Biostratigraphy after Agnini et al. (2011) following: (1) planktonic foraminiferal zones of Berggren and Pearson (2005) and (2) calcareous nannofossil zones of Martini (1971). Polarity/Chron (3) after Agnini et al. (2011). The hatched bands indicate intervals of marked carbonate dissolution.

with respect to organic input, under which they may become dominant faunal elements (e.g., Loubere, 1991; Gooday, 1996; Loubere, 1996; Loubere and Fariduddin, 1999a,b; Fontanier et al., 2002; Jorissen et al., 2007).

The C_{org} flux to the sea-floor directly influences the oxygenation at the sediment–water interface through oxidative degradation of organic matter: an excess of organic matter leads to lower oxygen availability to benthic communities (e.g., Valiela, 1984; Jorissen et al., 1995; Murray, 2006). Benthic foraminifera, as unicellular organisms, are in general able to tolerate oxygen depletion better than metazoans, and the more resistant taxa take advantage of a food-enriched environment where there is less competition (e.g., Phleger and Soutar, 1973; Koutsoukos et al., 1990; Sen Gupta and Machain-Castillo, 1993; Alve, 1995; Jorissen et al., 1995; Van der Zwaan et al., 1999). In most environments there thus is a strong, negative correlation between food supply and oxygen levels (TROX model, Jorissen et al., 1995). Interspecific competition influences the structure of benthic foraminiferal assemblages in

terms of abundance and species composition: the most diverse assemblages, combining epifaunal to fairly deep infaunal components, occur in environments which are neither extreme in food supply nor in oxygenation. At lower food levels there is not sufficient food to sustain infaunal populations although pore water oxygenation is good and would allow them to thrive, and at very high food supply the oxygen levels in pore waters (and finally in bottom waters) become too low to allow foraminifera to survive.

Knowledge of these relationships in the modern oceans helps to interpret fossil benthic foraminiferal assemblages, in order to gain information about past environmental changes. We are, however, limited in our understanding of past benthic foraminiferal assemblages by our limited knowledge of recent faunas. Even for many living species the relation between test morphology and microhabitat has not been observed directly, but is extrapolated from data on other taxa (e.g., Jorissen, 1999). This is necessarily so for extinct taxa. In addition, many foraminifera move vertically through the sediment (e.g., Gooday and Rathburn,

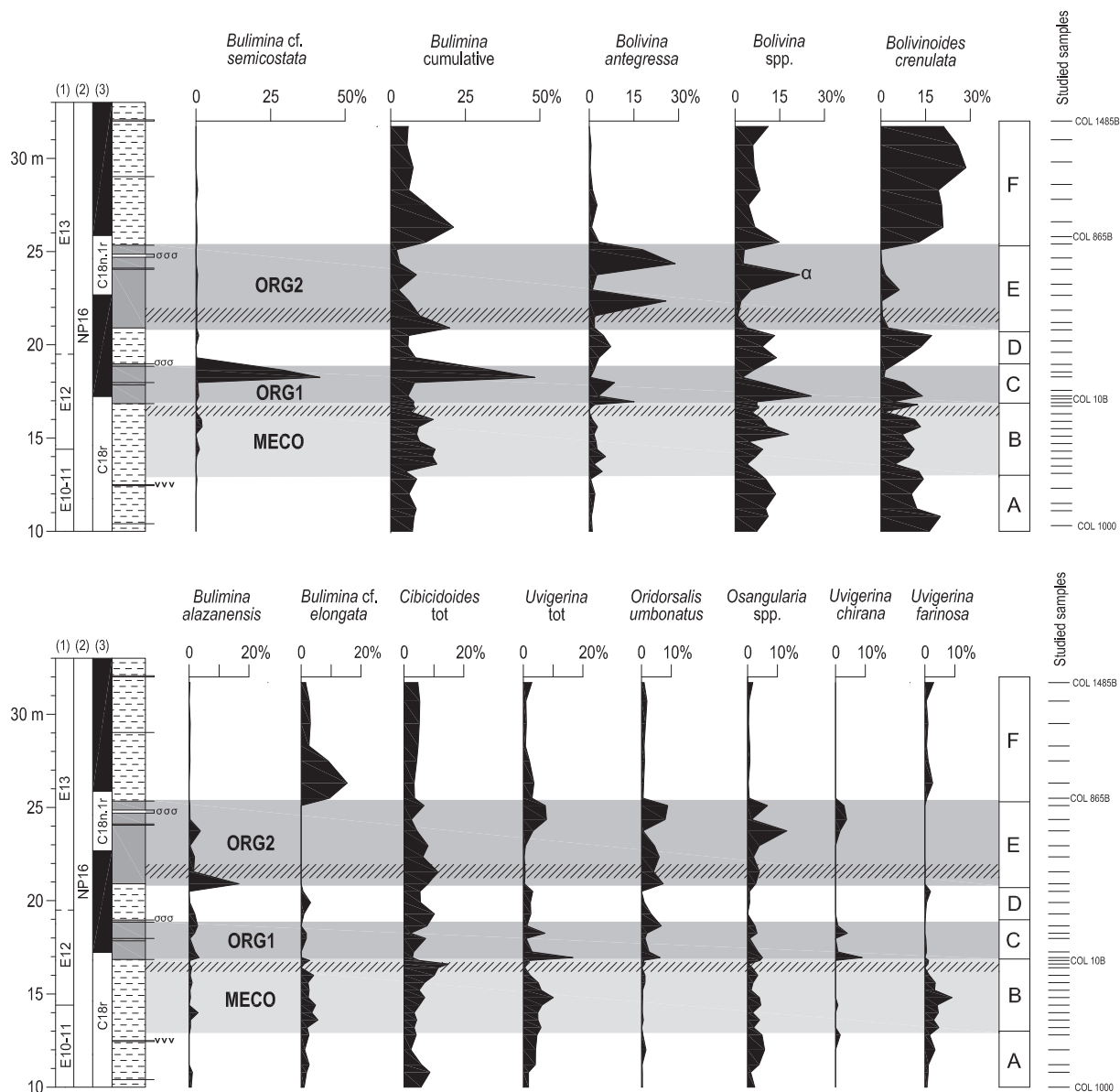


Fig. 3. Relative abundance of selected benthic foraminifera across the MECO in the Alano section plotted against bio-magnetostratigraphy, lithology and the recognized assemblages (A to F). The letter α indicates the ORG2 peak of *Bolivina nobilis*–*gracilis* transitional forms. Biostratigraphy after Agnini et al. (2011) following: (1) planktonic foraminiferal zones of Berggren and Pearson (2005) and (2) calcareous nannofossil zones of Martini (1971). Polarity/Chron (3) after Agnini et al. (2011). The hatched bands indicate intervals of marked carbonate dissolution.

1999; Fontanier et al., 2002). In one of the few statistical studies evaluating the correlation between test morphology and microhabitat, it is argued that the assignment of modern foraminifera to microhabitats may be accurate only about 75% (Buzas et al., 1993). Comparisons between past and recent environments thus need careful evaluation.

4. Results

Benthic foraminiferal assemblages at the Alano section are strongly dominated by calcareous forms throughout the studied interval (~85–98% of the assemblage; Fig. 2). There is a marked increase in the relative abundance of the agglutinated taxa in 2 samples just below the base of ORG1, and within samples from ORG2. The preservation of benthic foraminifera varies from good, in the lower and upper part of the section, to moderate, especially within the two ORG beds in which tests are filled by pyrite. In these intervals foraminifera are very rare in some samples.

4.1. Paleobathymetry

According to Agnini et al. (2011), the lower-middle portion of the Alano section, including the studied interval, was deposited at middle bathyal depth (600–1000 m, using depth distributions as in van Morkhoven et al., 1986). This estimate was based on the evaluation of P/B values (>90) and on the occurrence of paleobathymetric index taxa, including the presence of *Nuttallides truempyi*, *Cibicidoides barnetti* (indicative of depths > ~500–600 m), combined with taxa as *Hanzawaia ammophila* and *Oridorsalis umbonatus* (e.g., Ortiz and Thomas, 2006). The occurrence of common bi- and triserial taxa agrees with a middle bathyal depth assignment (Agnini et al., 2011).

4.2. Faunal changes across the Middle Eocene Climatic Optimum

Benthic foraminiferal assemblages show marked changes across the studied section, especially directly after the MECO, within the two ORG intervals and the directly overlying interval. Based on

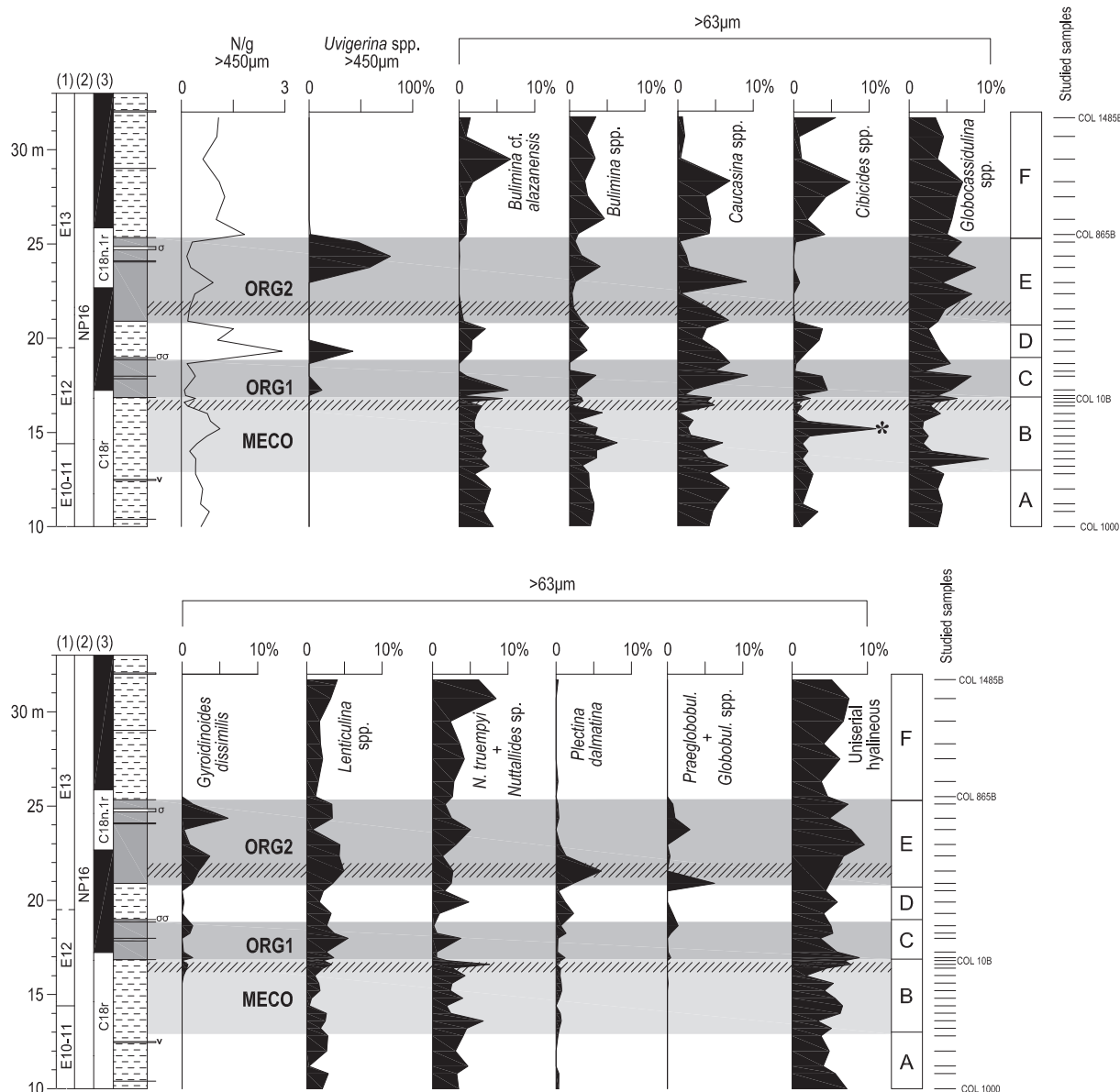


Fig. 4. N/g = number of benthic foraminifera per gram (faunal density), relative abundance of *Uvigerina* spp. heavy costate forms in the $\geq 450 \mu\text{m}$ size fraction and relative abundance of common benthic foraminiferal taxa in the $63 \mu\text{m} \leq 450 \mu\text{m}$ size fraction plotted against bio-magnetostratigraphy, lithology, stable isotopes ($\delta^{18}\text{O}$ and $\delta^{13}\text{C}$), $\text{CaCO}_3\%$ and total organic carbon (TOC%; from Spofforth et al., 2010). The asterisk * indicates the sample COL480A (15.20 m), in which anomalous high abundance of *Cibicides* spp. is associated with the presence of numerous resedimented specimens of shallow-water taxa belonging to the genera *Amphistegina*, *Asterigerina* and *Asterigerinata*. Biostratigraphy after Agnini et al. (2011) following: (1) planktonic foraminiferal zones of Berggren and Pearson (2005) and (2) calcareous nannofossil zones of Martini (1971). Polarity/Chron (3) after Agnini et al. (2011). The hatched bands indicate intervals of marked carbonate dissolution.

quantitative analysis, six main benthic foraminiferal assemblages (A to F; Fig. 2) were identified as described below.

4.2.1. Assemblage A: pre-MECO interval (5 samples, 10.00–12.80 m)

Samples below the onset of the MECO are characterized by fluctuating, moderately high faunal diversity (Fisher $\alpha \sim 24$) and absolute abundance around 350 specimens/g (Fig. 2). Infaunal taxa are more abundant (75%) than epifaunal, and consist of bi-triserial taxa (on average 33%, Table 1) and very small, weakly ornamented *Bolivinoidea crenulata* (on average 15%; Figs. 2, 3). Epifaunal taxa are represented mainly by *Nuttallides* spp. and *Cibicidoides* spp. (Figs. 3, 4). Preservation is moderately good, $\text{CaCO}_3\%$ is high ($\sim 45\%$) and the planktonic foraminiferal F-index is low, < 5 (Fig. 2; Table 1). At ~ 11 m, *B. crenulata* begins an upward decrease (both relative and absolute abundance), paralleled by a gradual increase in relative abundance of the other bi-triserial taxa (Fig. 3).

4.2.2. Assemblage B: MECO interval (11 samples, 13.20–16.80 m)

With the onset of MECO, the relative abundance of bi-triserial taxa increases upwards, reaching 40% (Fig. 2, Table 1). The genera *Bulimina* and *Uvigerina* increase in abundance to 13% and 8%, respectively. Among buliminids, *Bulimina stalacta*, *Bulimina* cf. *midwayensis*, the *Bulimina trinitatensis-impedens* group, *Bulimina* cf. *alazanensis*, and the *Bulimina* cf. *elongata* group become more common, as does the small, hispid, *Uvigerina farinosa* (Figs. 3, 4; Plate I). The foraminiferal assemblage becomes more diverse and structured, so that the Fisher- α index gradually increases to ~ 30 at the top of the interval (~ 15.60 m), with a richer agglutinated fauna (8%), mainly represented by large *Plectina dalmatina* and *Tritaxia szaboi* (Plate I). Among epifaunals, large, heavily calcified *Cibicidoides* spp., *Nuttallides truempyi* and the *Osangularia pteromphalia-mexicana* group are common (Figs. 3, 4; Plate II). *Plectina dalmatina*, *T. szaboi* and *Cibicidoides eocaenus* dominate the fraction $\geq 450 \mu\text{m}$. The total N/g and bi-triserial absolute abundance

Table 1
Typical values of parameters for the recognized benthic foraminiferal assemblages.

Assemblage	Fisher α	Dominance	N/g	Infaunal%	Bi-triserial%	F-index	CaCO ₃ %
F	19	0.184	550	~75	~30	9	45
E	~20	0.063	190	73	34	86	41
D	22	0.075	455	77	38	35	49
C	20	0.084	515	83	51	79	36
B	27	0.048	375	70	35	48	41
A	24	0.067	350	74	33	4	44
St.dev.	2.77	0.04	119.56	4.03	6.77	31.35	4.03

fluctuate throughout (Fig. 2). Close to the maximum $\delta^{18}\text{O}$ negative values (peak MECO) at the top of the interval, N/g peaks to the highest values (~900 specimens/g; ca. 15.40 m). The MECO acme at Alano (16.40–16.90 m) coincides with a drop in CaCO₃ (~30%), coarse fraction and peak F index values (80; Fig. 2), thus increased dissolution. Preservation of tests deteriorates, N/g drops to minimum values, and bi-triserial relative abundance and infaunal/epifaunal ratio markedly decrease (to ~24% and 57% respectively; Fig. 2). Agglutinated taxa peak at 25%, together with *Cibicides* spp. (~15%; Figs. 2, 3).

4.2.3. Assemblage C: post-MECO-ORG1 interval (5 samples, 16.95–18.65 m)

Within ORG1 (TOC ~2–3%; CaCO₃ ~35%), preservation of both benthic and planktonic foraminifera deteriorates, the F-index of planktonic foraminifera is around 80, and tests show signs of dissolution (Fig. 2). Both benthic and planktonic foraminifera are frequently filled with pyrite. The benthic foraminiferal assemblage changes dramatically: infaunal morphotypes become dominant, with percentages close to 85%. Bi-triserial taxa reach their highest values (around 50%), whereas the relative and absolute abundance of *Bolivinoidea crenulata* decreases at the top of the interval, after a series of fluctuations (Figs. 2, 3). Benthic foraminiferal absolute abundance is high (~500 specimens/g), while Fisher α decreases (~20; Fig. 2, Table 1). The ORG1 interval is characterized, from the bottom to the top, by a series of peaks of different buliminids (Fig. 3): *Uvigerina* spp. and *Uvigerina chirana* (together ~20%), *Bolivina antegressa* (15%), small *Bolivina* spp. (~30%), *B. crenulata* (~13%) and *Bulimina cf. semicostata* (~35%) (Plate I, Appendix C). The ORG1 interval is lithologically heterogeneous: it is interrupted at 17.98 m (sample COL113B) by a thin, greenish layer with a lower TOC% content (Fig. 2). In this layer, the benthic foraminiferal assemblage differs from that in underlying and overlying samples, because the percentage of bi-triserial taxa and the infaunal/epifaunal ratio drop to values similar to that of the pre-MECO interval (40% and 70% respectively; Fig. 2), although the absolute abundance of these taxa is still high. *Bolivinoidea crenulata* shows a slight increase, to up to 8% (Fig. 3).

4.2.4. Assemblage D: marly interval between ORGs (4 samples, 19.30–20.50 m)

The faunal composition of Assemblage D resembles that in the pre-MECO interval, and in sample COL113B (ORG1 at 17.98 m). General preservation of both benthic and planktonic foraminifera improves (F-index ~35, CaCO₃ ~50%; Fig. 2, Table 1), the infaunal/epifaunal value drops to ~75%, and bi-triserial taxa, despite the high absolute abundance, are ~40% and mainly represented by small bolivinids (Fig. 3).

Bolivinoidea crenulata attains a percentage around 15%, total N/g is on average 450 specimens/g and Fisher α is ~22 (Figs. 2, 3).

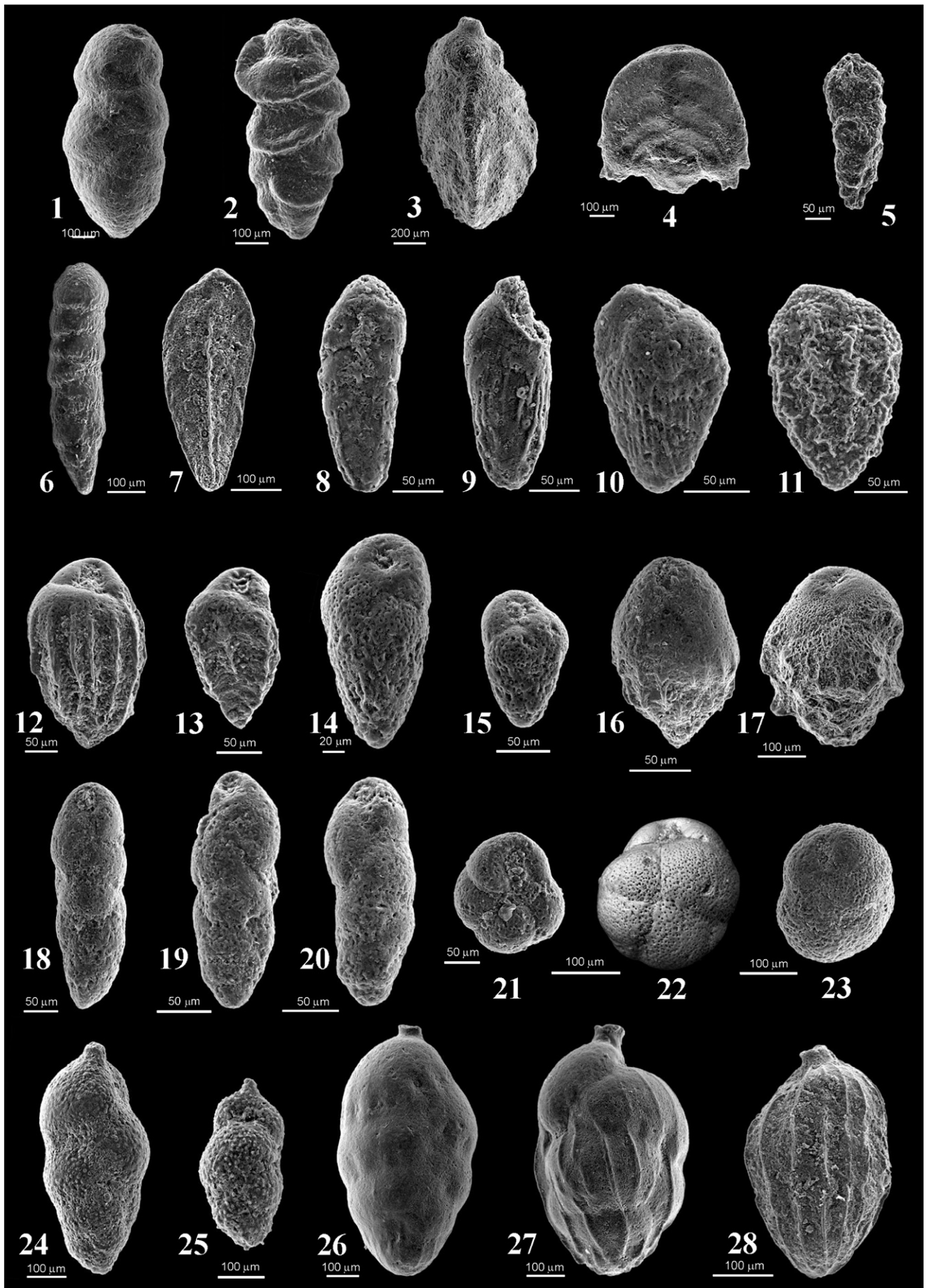
4.2.5. Assemblage E: post-MECO ORG2 interval (7 samples, 20.90–25.10 m)

Within the ORG2 interval CaCO₃ drops again (41%), the preservation of foraminifera is markedly worse than in interval ORG1, dissolution is more marked, and the F-index is slightly higher (Fig. 2, Table 1). ORG2 is similar to ORG1 in its high percentages of bi-triserial taxa and infaunal morphotypes (Fig. 2, Table 1). As in ORG1, buliminids peak (Figs. 3, 4) such as *Bulimina alazanensis* (17%), as do some biserial species, such as *Bolivina antegressa* (double peak of 26 and 29%), *Bolivina nobilis-Bolivina gracilis* transitional forms (21%), and to a lesser extent *Uvigerina* spp. (7%) (Plate I; Appendix C). Typical for this interval are increases in small osangulariids (peak to 13%; Fig. 3 and Plate II), *Oridorsalis umbonatus* (Fig. 3; Plate II) and calcareous uniserial taxa. ORG2 mainly differs from ORG1 by its markedly lower absolute abundance of benthic foraminifera (from 500 to ca. 200 specimens/g on average; Fig. 2, Table 1). Bi-triserial and infaunal taxa are less abundant in ORG2 than in ORG1, fluctuating between 20–35 and 70–80% respectively, and faunal diversity fluctuates strongly in the lower-middle portion, whereas in the upper part it remains more or less stable, around 15 (Fig. 2). Higher Fisher α values are recorded in 2 samples at 21.55 and 22.95 m (samples COL470B and 610B). In the lower one the high faunal diversity (Fig. 2) is associated with increased agglutinated foraminiferal abundance (mainly plectinids, Fig. 4), the upper one corresponds to a grey-greenish, organic poor marly layer. Both these samples have a lower percentage of bi-triserial taxa and infaunal/epifaunal ratio (Fig. 2), and COL610B shows a slight increase in abundance of *Bolivinoidea crenulata* (both relative and absolute abundance, Figs. 2, 3).

4.2.6. Assemblage F: recovery phase after the post-MECO interval (7 samples; 25.50–31.70 m)

Assemblage F coincides with the full recovery to pre-event values in $\delta^{18}\text{O}$ and $\delta^{13}\text{C}$ records, as well as in CaCO₃ (45%) and TOC percentages. The preservation of foraminifera is good, and the F-index has very low values (Fig. 2, Table 1). Assemblage F is characterized by an increase in N/g (>500 specimens/g) reflecting the highest faunal density of the studied interval (Table 1), mainly specimens of *Bolivinoidea crenulata* (100–150 specimens/g). The relative abundances of *B. crenulata* and other bi-triserial taxa are high (20–30% and 40%, respectively). *Bolivinoidea crenulata* continues to increase in abundance up to the top of the assemblage, whereas the other buliminids decrease markedly. Bi-triserial taxa are mainly represented by very small, smooth-walled

Plate I. Fig. 1 *Plectina dalmatina* (Schubert, 1911) COL140B-18.25 m; Fig. 2 *Plectina* sp. COL10B-16.95 m; Fig. 3 *Tritaxia szabo*i (Hantken, 1875) COL440A-14.80 m; Fig. 4 *Vulvulina eocaena-haeringensis* group COL865B-25.50 m; Fig. 5 *Eobigenerina variabilis* (Vašiček, 1947) COL520A-15.60 m; Fig. 6 *Rectouvigerina mexicana* (Cushman, 1926) COL470B-21.55 m; Fig. 7 *Bolivina antegressa* Subbotina, 1953 COL945B-26.30 m; Fig. 8 *Bolivina nobilis-gracilis* transitional forms COL690B-23.75 m; Fig. 9 *Bolivina nobilis-gracilis* transitional forms COL690B-23.75 m; Fig. 10 *Bolivina* sp. smooth/slightly costate group; Fig. 11 *Bolivinoidea crenulata* (Cushman, 1936) COL945B-26.30 m; Fig. 12 *Bulimina alazanensis* Cushman, 1927 COL405-20.90 m; Fig. 13 *Bulimina cf. alazanensis* Cushman, 1927 COL520A-15.60 m; Fig. 14 *Bulimina cf. semicostata* Nuttall, 1930 COL140B-18.25 m; Fig. 15 *Bulimina cf. semicostata* Nuttall, 1930 COL140B-18.25 m; Fig. 16 *Bulimina stalacta* Cushman and Parker, 1936 COL560A-16.00 m; Fig. 17 *Bulimina trinitatis-impedens* group COL470B-21.55 m; Fig. 18 *Bulimina cf. elongata* d'Orbigny, 1846 group COL440A-14.80 m; Fig. 19 *Bulimina cf. elongata* d'Orbigny, 1846 group COL945B-26.30 m; Fig. 20 *Bulimina cf. elongata* d'Orbigny, 1846 group COL945B-26.30 m; Fig. 21 *Caucasina* sp. COL1065B-27.50 m; Fig. 22 *Globocassidulina subglobosa* (Brady, 1881) COL140B-18.25 m; Fig. 23 *Globocassidulina punctata* Berggren and Miller, 1986 COL80A-11.20 m; Fig. 24 *Uvigerina chirana* Cushman and Stone, 1947 COL10B-16.95 m; Fig. 25 *Uvigerina farinosa* Hantken, 1875 COL440A-14.80 m; Fig. 26 *Uvigerina* sp. A COL10B-16.95 m; Fig. 27 *Uvigerina* sp. C COL10B-16.95 m; Fig. 28 *Uvigerina* sp. heavy costate form COL245B-19.30 m.



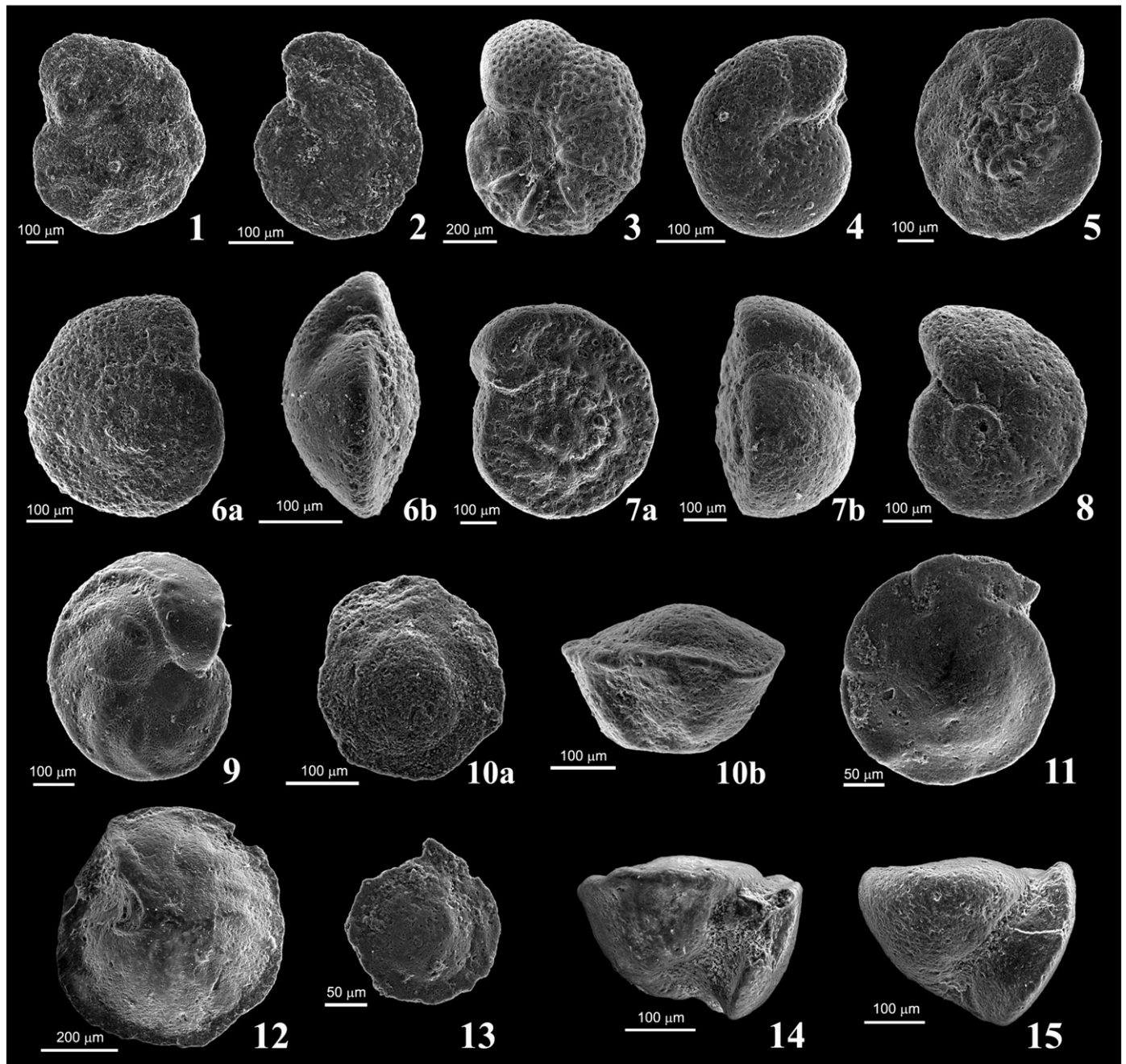


Plate II. Fig. 1 *Reticulophragmium* cf. *acutidorsatum* (Hantken, 1868) COL825B-25.10 m; Fig. 2 *Haplophragmoides walteri* (Grzybowski, 1898) COL945B-26.30 m; Fig. 3 *Anomalinoidea capitatus* (Gümbel, 1868) COL520A-15.60 m; Fig. 4 *Anomalinoidea spissiformis* Cushman and Stainforth, 1945 COL305B-19.90 m; Fig. 5 *Cibicidoides ungerianus* (d'Orbigny, 1846) COL440A-14.80 m; Fig. 6a *Cibicidoides eoacaenus* (Gümbel, 1868) spiral view COL1000-10.00 m; Fig. 6b *Cibicidoides eoacaenus* (Gümbel, 1868) lateral view COL365B-20.50 m; Fig. 7a *Cibicidoides grimsdalei* (Nuttall, 1930) spiral view COL945B-26.30 m; Fig. 7b *Cibicidoides grimsdalei* (Nuttall, 1930) spiral view COL945B-26.30 m; Fig. 8 *Cibicidoides micrus* Bermúdez, 1949 COL500A-15.40 m; Fig. 9 *Hanzawaia ammophila* Gümbel, 1868 COL40B-17.25 m; Fig. 10a *Nuttallides truempyi* (Nuttall, 1930) spiral view COL1000-10.00 m. Fig. 10b *Nuttallides truempyi* (Nuttall, 1930) lateral view COL440A-14.80 m; Fig. 11 *Oridorsalis umbonatus* (Reuss, 1851) spiral view COL750B-24.35 m; Fig. 12 *Osangularia pteromphalia-mexicana* group umbilical view COL440A-14.80 m; Fig. 13 *Osangularia* sp. spiral view COL690B-23.75 m; Fig. 14 *Gyroidinoides dissimilis* (Cushman and Renz, 1947) COL140B-18.25 m; Fig. 15 *Gyroidinoides soldanii* d'Orbigny, 1826 COL520-15.60 m.

or weakly costate bolivinids and by very small and smooth-walled *Bulimina*, mainly the *Bulimina* cf. *elongata* group (average 13%; Fig. 3).

5. Discussion

5.1. Pre-MECO and MECO (assemblages A, B): toward increased food availability at the sea floor

In the Alano section, pre-MECO background conditions (assemblage A) are characterized by a fairly abundant and diversified infauna, with

abundant small bolivinids including *Bolivinoidea crenulata* (Figs. 2, 3). The abundance of bi-triserial taxa indicates a high and continuous food supply to the sea-floor (e.g., Gooday and Rathburn, 1999; Loubere and Fariduddin, 1999b; Morigi et al., 2001; Gooday, 2003). The common occurrence of buliminids in assemblage A, however, probably cannot be ascribed to very high productivity in the surface waters. The scarce epifaunal community, and the low diversity and low abundance assemblage, coupled with absence of evidence for hypoxic conditions (Spofforth et al., 2010), suggest that there was a low to moderate flux of organic matter to the seafloor, as supported by calcareous plankton

communities indicating generally oligotrophic surface waters (Luciani et al., 2010; Toffanin et al., 2011). The apparent mismatch between benthic foraminifera indicative of a higher organic supply than suggested by indicators of productivity in overlying waters can be explained by the presence of an additional, lateral supply of more refractory organic matter (e.g., as in the present bay of Biscay, Fontanier et al., 2005), especially in view of the paleogeographic setting of the Alano section, i.e., the vicinity of land and the shelf areas surrounding the Belluno basin. This setting may have allowed a supply of terrigenous material containing refractory organic matter (e.g., Ortiz and Thomas, 2006). Some infaunal taxa are able to use such refractory organic matter (e.g. Fontanier et al., 2002, 2005). Bolivinids specifically are characterized by tolerance to a wide spectrum of trophic and oxygen conditions (e.g. Kitazato and Ohga, 1995; Silva et al., 1996; Bernhard et al., 1997). We therefore argue that benthic foraminiferal data from the pre-MECO interval may indicate relatively oligotrophic surface waters, under which the sea floor habitat was influenced by continental-derived, refractory organic matter.

With the beginning of the MECO, the relative abundance of bi- and triserial taxa started to increase (assemblage B), suggesting a gradual increase in supply of less refractory organic material from increased primary productivity in overlying surface waters. The relative abundance of bi-triserial taxa, indicative of a continuous food supply (e.g. Lutze and Coulbourn, 1984), increased together with faunal diversity. Within the samples just below the maximum negative OIE (i.e. peak MECO), peak values in benthic foraminiferal absolute abundance were reached (Fig. 2). Such an increase in benthic foraminiferal absolute abundance may indicate the supply of larger amounts or less refractory organic matter to the benthos (Herguera and Berger, 1991; Jorissen et al., 1995; Thomas et al., 1995; Gooday, 2003; Jorissen et al., 2007). Among bi-triserial taxa, small and hispid uvigerinids such as *Uvigerina farinosa* increased in abundance (Fig. 3). These forms resemble living *Uvigerina* species typical for deep-sea high productivity areas (Loubere, 1991, 1996, 1997; Loubere and Fariduddin, 1999b). N/g can be influenced by the abundant presence of small individuals and decreased sedimentation rates (Thomas, 2003; Giusberti et al., 2009), but that is not the case here: in assemblage B, the abundance of the coarse fraction and the mean size of benthic foraminiferal tests increase, and sedimentation rates increase (Spofforth et al., 2010).

The N/g values in assemblage B increase, coupled with a gradual increase in influx of detrital material (Spofforth et al., 2010), and a shift from oligotrophic to more eutrophic-dominated calcareous planktonic communities (Luciani et al., 2010; Toffanin et al., 2011). This increased influx of terrestrial detrital sediments may have resulted from increased weathering resulting from the increasingly vigorous hydrological cycle during warm climates (Pierrehumbert, 2002). The increased delivery of highly weathered, inorganic terrestrial material may have provided more nutrients, resulting in higher surface productivity (Luciani et al., 2010; Spofforth et al., 2010; Toffanin et al., 2011). The latter led to intensified export productivity to the sea floor and thus a higher supply of labile, more nutritious fresh phytal material to the benthos.

The high faunal diversity across the MECO (Fig. 2, Table 1) indicates that the higher flux of labile organic matter, though able to sustain a richer infaunal and epifaunal community, did not result in poorly oxygenated conditions (e.g. Jorissen et al., 1995; Levin et al., 2001; Gooday, 2003). Overall, the benthic foraminiferal data provide evidence for a transition from more oligotrophic conditions with lateral supply of terrestrial organic matter to a fully mesotrophic environment favouring exploitation of both infaunal and epifaunal ecological niches, thus establishment of a more complex and vertically structured benthic foraminiferal community (e.g., Jorissen et al., 1995; Van der Zwaan et al., 1999).

An exception to the increase in biserial-triserial taxa was the decrease in abundance of the biserial species *Bolivinoidea crenulata* during the onset of the MECO, although with, strong fluctuations (Figs. 2, 3). This species thus shows a trend in abundance opposite to that of the other bi-triserial taxa. Possibly, this taxon could outcompete

other infaunal taxa at a higher abundance of refractory organic matter and lesser abundance of freshly produced phytal material. Alternatively, it could not compete well under higher temperatures, as it also decreased in abundance during a hyperthermal event at the early/middle Eocene boundary in middle bathyal section Agost, Spain (Ortiz et al., 2008).

The MECO peak-warming at Alano coincided with a marked drop in the preservation of foraminiferal tests, which show pitting, thus signs of dissolution, a drop in N/g values, coarse fraction and in CaCO₃%, thus overall carbonate dissolution (Fig. 2). As a result of dissolution, bi-triserial taxa strongly declined in absolute abundance, and peak values in Fisher α diversity declined, while the relative abundance of the dissolution-resistant *Cibicidoides* spp. and agglutinated taxa increased (Figs. 2, 3). The presence of a dissolution interval during MECO at the relatively shallow setting of the Alano section (600–1000 m) probably does not reflect a global rise in the lysocline. Bohaty et al. (2009) did not observe severe dissolution even at depths greater than 3000 m, where the mass accumulation of CaCO₃ declined, and at shallower depths even the mass accumulation rates of CaCO₃ remained unchanged. Our data thus indicate that the lysocline shallowed considerably during MECO at a regional scale in the western Tethys, while much less shallowing occurred in the Atlantic and Pacific oceans. Further paleoceanographic studies on the Eocene Tethys are needed in order to test in which regions there is evidence for a rising lysocline.

5.2. Post-MECO ORG1 (assemblage C): eutrophication and hypoxia at the sea-floor

Striking paleoceanographic changes occurred at Alano immediately after the peak temperatures of MECO were reached. Within this interval, relatively high benthic foraminiferal absolute abundance, high percentage and N/g of mostly small bi-triserial taxa (Figs. 2, 3), suggest that the dissolution affecting the assemblage was minor and did not compromise the overall ecological signal (Table 1).

Benthic foraminiferal assemblage C has high N/g values, a lower diversity (Fisher alpha) than its predecessor faunas, due to the strong dominance of infaunal morphotypes (*Bulimina*, *Bolivina* and *Uvigerina*), with high percentages of bi-triserial taxa (Figs. 2, 3, 4), suggesting a eutrophic sea-floor environment with a high, continuous flux of organic matter (e.g., Lutze and Coulbourn, 1984; Jorissen et al., 1995; Morigi et al., 2001; Gooday, 2003). In the modern oceans, these genera dominate assemblages under high food and low oxygen conditions (e.g., Sen Gupta and Machain-Castillo, 1993; Alve and Bernhard, 1995; Bernhard and Sen Gupta, 1999), such as those during deposition of the Neogene and Quaternary Mediterranean sapropels (e.g., Katz and Thunell, 1984; Jorissen, 1999; Schmiedl et al., 2003; Morigi, 2009). Buliminids are tolerant to hypoxic conditions and able to take advantage from the large amounts of organic matter and low interspecific competition that generally characterize oxygen-poor environments (e.g., Sen Gupta and Machain-Castillo, 1993; Alve, 1995; Bernhard et al., 1997; Van der Zwaan et al., 1999; Gooday, 2003). Assemblage C thus may indicate oxygen depletion at the sea floor, or at least within pore waters close to the seafloor to which infaunal taxa are exposed. Oxygen levels probably fell below the tolerance of the more oxiphilic species (e.g., Van der Zwaan et al., 1999; Gooday, 2003; Jorissen et al., 2007), but remained above the threshold for infaunal taxa (≤ 1 ml/l; Murray, 2001). The entire interval is bioturbated and benthic foraminifera occur throughout, thus the interval is not characterized by anoxia, but the geological record is always time-averaged, so that we cannot exclude that brief (e.g., millennial or submillennial) episodes of anoxia occurred, but directly followed by recolonization of the benthos. The hypoxic conditions may have been exacerbated by increased fresh water influx into the basin due to the increased vigour of the hydrological cycle during the warm peak of MECO (e.g., Pierrehumbert, 2002).

The striking change in the benthic foraminiferal composition during the transition from assemblage B to assemblage C can be explained as caused by a food-enriched, somewhat oxygen depleted sea-floor environment, which favoured a fairly diversified “high productivity”, stress-tolerant fauna. Sedimentological and geochemical proxies support this hypothesis, because the high TOC% values, common occurrence of pyrite, low Mn/Al and high S% indicate oxygen-poor conditions at or just below the sea-floor (Spofforth et al., 2010). The benthic foraminiferal evidence indicates, however, that the hypoxic conditions were not stable: within assemblage C, peaks of different species of buliminids occur (Fig. 3). For example, the sample dominated by *Bolivinooides crenulata* (COL40B-17.25 m) and other bolivinids abundant in the underlying assemblages, indicates a lower flux of organic matter and a better oxygenation at the sediment/water interface, than the surrounding samples (Fig. 3). Similar instability is shown in the occurrence of the light-coloured, marly layer within ORG1 (sample COL113B-17.98 m), also dominated by *B. crenulata* (Figs. 2, 3), and with a lower infaunal/epifaunal ratio and bi-triserial taxa percentage, suggestive of a significant lowering of the flux of organic matter and temporary re-oxygenation at the sediment/water interface. Geochemical and sedimentological proxies agree with this interpretation (Spofforth et al., 2010).

We thus speculate that a strong competition for resources at and just below the sediment/water interface influenced the composition of the benthic assemblages, favouring peaks of diverse taxa depending on the degree of organic flux and oxygen depletion, thus motion of redox boundaries through the sediment column (e.g., Van der Zwaan et al., 1999; Fontanier et al., 2005; Jorissen et al., 2007). In conclusion, we infer that variable and fluctuating C_{org} flux regimes characterized ORG1 deposition, indicating an unstable paleoenvironment with variable surface waters productivity.

5.3. Marly interval between ORGs (assemblage D): improved bottom water oxygenation and decreasing surface productivity

The benthic assemblages in this organic poor interval indicate re-oxygenation linked to a significant decrease in surface water productivity, and potentially some cooling, as indicated by the abundance of *Bolivinooides crenulata* and the decrease of the eutrophic, low-oxygen tolerant taxa, particularly in the middle-upper part of the interval (Figs. 2, 3). High infaunal/epifaunal values persist and a high abundance of bi-triserial taxa (relative and absolute) coupled with high total N/g values (Fig. 2) occur at the base of this interval. These data, along with maximum values of absolute and relative abundance of heavily costate *Uvigerina* spp. in the $\geq 450 \mu\text{m}$ fraction (Fig. 4; Plate I), indicate that the flux of organic matter was still high, and relatively continuous. The high diversity, however, suggests that higher oxygen levels returned at the sediment/water interface, as corroborated by sedimentological evidence. The persistent high total N/g (Fig. 2) may be caused by an increase in abundance of small specimens, and/or by the decreased sedimentation rate of detrital input (Spofforth et al., 2010). Benthic assemblages agree with the interpretation of changes in calcareous plankton indicating an overall decrease of eutrophication (Luciani et al., 2010; Toffanin et al., 2011).

5.4. Post-MECO ORG2 (assemblage E): increased hypoxia at the sea-floor

During the deposition of ORG2 surface water productivity increased again, leading to a higher C_{org} flux to the sea floor as indicated by increase of bi-triserial taxa (Figs. 2, 3), and the dark colour of the marls due to high TOC. Benthic foraminiferal preservation declined in assemblage E, while F-index values increased (Fig. 2), indicating increased carbonate dissolution, even somewhat higher than in ORG1. The dissolution does not seem to have significantly altered the benthic foraminiferal signal in most samples, as shown by the constant presence of small specimens (e.g., bolivinids, osangulariids, *Globocassidulina* spp.; Figs. 3, 4). Sample COL470B (+21.55 m) is an exception, and has poor

preservation associated with high faunal diversity, low faunal density and bi-triserial abundance, and a high agglutinated/hyaline value (Figs. 2, 3). The high faunal diversity is caused by removal of the small and dominant buliminids by dissolution, thus emphasizing the abundance of other taxa, mostly agglutinants (Figs. 2, 4).

The benthic foraminiferal signal might have been affected by carbonate dissolution, but overall assemblage E indicates more severely oxygen-depleted conditions during ORG2 deposition than during ORG1. The lowermost portion of this interval (COL405B-20.90 m) is characterized by a high abundance of *Bulimina alazanensis* (Fig. 3), a typical taxon of modern oceans “high productivity” assemblages (Loubere, 1991, 1996, 1997; Loubere and Fariduddin, 1999b). High primary productivity leading to lowered oxygen conditions is indicated by the taxonomic composition of the foraminiferal assemblage, which is dominated by very small bolivinids such as *Bolivina antegressa* and *Bolivina nobilis*–*Bolivina gracilis* group, associated with abundant small *Osangularia* spp. (Fig. 3). *Osangularia* is common in many Cretaceous black shales, and considered an opportunistic taxon able to rapidly recolonize when oxygenation improves slightly (e.g., Friedrich et al., 2005).

The small bolivinids are morphologically similar to those dominating assemblages in the oxygen minimum zones (OMZs) in the present Pacific and Indian Oceans (e.g., *Bolivina argentea* and *Bolivina seminuda*; Sen Gupta and Machain-Castillo, 1993; Bernhard et al., 1997). Small calcareous benthic foraminifera typically dominate assemblages in oxygen-depleted environments (e.g., Koutsoukos et al., 1990). *Bolivina* in hypoxic sediments may be small as the result of physiological adaptation for facilitating gas exchange (e.g., Bernhard et al., 2010), and the small size minimizes oxygen consumption with respect to the surface-to-volume ratio (Bradshaw, 1961; Kuhnt and Wiedmann, 1995; Friedrich, 2009). In addition, opportunistic benthic foraminifera tend to reproduce fast (thus at an early age and small size) under low oxygen conditions, due to the low competition at high food availability (Phleger and Soutar, 1973; Koutsoukos et al., 1990; Friedrich, 2009). The low oxygen conditions due to high surface primary productivity may have been exacerbated by increased fresh water flux into the basin due the increased vigour of the hydrological cycle during warm climates (e.g., Pierrehumbert, 2002).

We thus argue that only the most opportunistic taxa could thrive to form the low-diversity high-dominance Assemblage E (e.g., Koutsoukos et al., 1990; Jorissen et al., 1995; Van der Zwaan et al., 1999). Geochemical proxies also indicate more markedly hypoxic conditions during ORG2 than during ORG1 at Alano (Spofforth et al., 2010), as also suggested by the highest abundance of the deep infaunal *Praeglobobulimina*, *Globobulimina* species in the studied section. Lower N/g in the assemblage might have been caused by hypoxia, but could also have been influenced by enhanced dissolution caused by pore water acidification due to excessive organic decay and pyrite oxidation (e.g., Green et al., 1993; Aller and Blair, 2006; Sprong et al., 2012). Different degrees of preservation in ORG2 suggest the occurrence of brief re-oxygenation episodes of varying duration and intensity (e.g., Green et al., 1993; Diester-Haass et al., 1998). Such episodes of reventilation could have been associated with less productive surface waters, such as reflected in sample COL610B (22.95 m), an organic poor, light-coloured layer with common *Bolivinooides crenulata*, high Fisher α , low dominance and bi-triserial percentage (Figs. 2, 3).

In conclusion, the structure and composition of assemblage E reflect high productivity and low oxygen conditions, under unstable water column stratification, leading to variability in the degree of oxygenation and flux of organic matter at the sea floor.

5.5. Recovery phase above post-MECO (assemblage F): rapid sea-floor re-oxygenation and return to background conditions

Directly above ORG2, benthic foraminifera abruptly return to a higher faunal density (Table 1) and became dominated by *Bolivinooides*

crenulata, together with small and little ornamented bi-triserial taxa such as *Bulimina cf. elongata* and *Bulimina cf. alazanensis* (Appendix C), which are more abundant in assemblage F than in the pre-MECO interval (Figs. 2, 3, 4). When oxygenation recovered, and possibly waters cooled assisting in recovery of oxygenation, *B. crenulata* and other bi-triserial taxa took advantage of the increased oxygen availability and the organic matter stored in the sediments, reaching higher abundances than in assemblage A. If sedimentation was continuous, the abrupt disappearance of taxa typical for hypoxic conditions just above the uppermost dark marls testifies to a very rapid return to well-oxygenated bottom waters, as well as normally productive surface waters for the region. Such rapid reoxygenation may have been assisted by decreasing density gradients in the water column due to the decrease in fresh-water supply at the end of the MECO warm period, as well as by the decreasing temperatures.

6. Summary and conclusions

- (1) Benthic foraminiferal assemblages indicate that in the Alano section in western Tethys environments gradually changed toward more eutrophic conditions at the onset of the MECO, culminating with the deposition of the two sapropelic intervals after the end of peak-MECO warming, in agreement with the observed marked increase in abundance of eutrophic–opportunistic taxa of calcareous plankton in these intervals (Luciani et al., 2010; Spofforth et al., 2010; Toffanin et al., 2011).
- (2) The marine productivity may have gradually increased as a response to increase in fresh-water run-off during increased vigour of the hydrological cycle during MECO warming, which augmented influx of nutrients from increased weathering, thus higher nutrient availability, leading to increased surface and export productivity, and increased the quality and quantity of organic matter reaching the sea-floor.
- (3) Micropaleontological, geochemical, isotopic and sedimentological data all indicate that the environment at the Alano section was unstable and perturbed throughout the post-MECO interval when two layers of organic-rich sediment were deposited, probably under hypoxic conditions (Luciani et al., 2010; Spofforth et al., 2010; Toffanin et al., 2011).
- (4) Benthic foraminiferal data present evidence that this instability was expressed in an increase in surface productivity during deposition of the organic rich layers, thus increasing the C_{org} flux which led to lower bottom water oxygenation and increased organic matter preservation. Such changes in surface-water productivity could be explained by an intermittently strengthened hydrological cycle leading to overall increased but variable delivery of nutrients.
- (5) A transient interval of lowered surface productivity interrupted the deposition of organic rich sediment, as shown by a decrease in abundance of planktonic and benthic foraminiferal taxa. Benthic foraminifera indicate that the reduced primary productivity was coupled to improved bottom water oxygenation, possibly during cooler, less humid conditions.
- (6) Biotic, sedimentological and geochemical data suggest that after this transient interval, hypoxic conditions returned during deposition of the second organic rich layer, due to increasing surface water productivity caused by renewed fresh water influx carrying nutrients. Benthic foraminiferal assemblages indicate a more stressed, more-oxygen depleted sea-bottom environment than during the deposition of the first organic-rich layer.
- (7) The deposition of the organic rich layers was local or regional, but its occurrence just after the MECO peak warming may suggest a connection, possibly through passing of an environmental threshold. The rapid increase in temperature during the MECO-peak warming could have caused increased discharge of nutrient-rich fresh waters into the basin, thus highly increased productivity, especially because the Alano section

was located relatively close to the end of the basin, limiting bottom-surface water exchange.

- (8) Benthic foraminiferal data combined with the record of calcareous plankton (Luciani et al., 2010; Toffanin et al., 2011), provide clear evidence that the increased productivity caused the positive carbon isotope excursion during deposition of the organic rich layers at Alano, because of the burial of isotopically light organic matter (Luciani et al., 2010; Spofforth et al., 2010).
- (9) The Alano record thus may support the hypothesis by Bohaty et al. (2009) that increased organic carbon burial could have acted to sequester an excess of CO_2 from the ocean–atmosphere system in a relatively short time interval (Spofforth et al., 2010), possibly in combination with organic carbon burial in other marginal basins (Beniamovski et al., 2003).
- (10) The MECO and post-MECO intervals were not associated with extinctions or permanent changes in the structure and composition of the benthic foraminiferal communities in the middle bathyal setting in western Tethys.
- (11) Studies of the biotic effects of MECO are needed at more locations in order to provide a more global perspective of the event, allowing a better understanding of the benthic foraminiferal response to this transient warm period of Earth history.

Supplementary data to this article can be found online at <http://dx.doi.org/10.1016/j.palaeo.2013.03.018>.

Acknowledgments

F.B.G. thanks A. Asioli for precious advices and valuable discussions. F.B.G. and L.G. were financially supported by Padova University (Progetto di Ateneo GIUSPRAT10). This paper greatly benefited from the constructive comments by two anonymous referees and by the Editor Thierry Corrège. Thanks are due to Lorenzo Franceschin for processing supplementary samples. SEM images were acquired at the C.U.G.A.S (Centro Universitario Grandi Apparecchiature Scientifiche) of the Padova University. E.T. thanks the Leverhulme Trust for funding her stay at the University of Bristol as Visiting Professor.

References

- Agnini, C., Fornaciari, E., Giusberti, L., Grandesso, P., Lanci, L., Luciani, V., Muttoni, G., Rio, D., Stefani, C., Pálfi, H., Spofforth, D.J.A., 2011. Integrated bio-magnetostratigraphy of the Alano section (NE Italy): a proposal for defining the Middle–Late Eocene boundary. *Geological Society of American Bulletin* 123 (5/6), 841–872. <http://dx.doi.org/10.1130/B30158.1>.
- Aller, R.C., Blair, N.E., 2006. Carbon remineralization in the Amazon–Guiana tropical mobile mudbelt: a sedimentary incubator. *Continental Shelf Research* 26, 2241–2259.
- Alve, E., 1995. Benthic foraminiferal distribution and recolonization of formerly anoxic environments in Drammensfjord, southern Norway. *Marine Micropaleontology* 25, 169–186.
- Alve, E., Bernhard, J.M., 1995. Vertical migratory response of benthic foraminifera to controlled oxygen concentrations in an experimental mesocosm. *Marine Ecology Progress Series* 116, 137–151.
- Barbieri, R., 1990. L'Eocene medio e superiore del Bacino di Tripolitania (Libia nord occidentale): biostratigrafia e paleoecologia. *Bollettino della Società Paleontologica Italiana* 29 (3), 253–271.
- Beniamovski, V.N., Alekseev, A.S., Ovechkina, M.N., Oberhänsli, H., 2003. Middle to Upper Eocene disoxic–anoxic Kuma Formation (northeast Peri-Tethys): biostratigraphy and paleoenvironments. In: Wing, S.L., Gingerich, P.D., Schmitz, B., Thomas, E. (Eds.), *Causes and Consequences of Globally Warm Climates in the Early Paleogene*: Boulder, Colorado, Geological Society of America Special Paper, 369, pp. 95–112.
- Berggren, W.A., Pearson, P.N., 2005. A revised tropical to subtropical Paleogene planktonic foraminiferal zonation. *Journal of Foraminiferal Research* 35, 279–298.
- Berggren, W.A., Kent, D.V., Swisher III, C.C., Aubry, M.-P., 1995. A revised Cenozoic geochronology and chronostratigraphy. In: Berggren, W.A., et al. (Ed.), *Geochronology, Time Scales and Global Stratigraphic Correlation*: Society for Sedimentary Geology Special Publication, 54, pp. 129–212.
- Bernhard, J.M., Sen Gupta, B.K., 1999. Foraminifera of oxygen-depleted environments. In: Sen Gupta, B.K. (Ed.), *Modern Foraminifera*. Kluwer Academic Press, pp. 201–216.
- Bernhard, J.M., Sen Gupta, B.K., Borne, P.F., 1997. Benthic foraminiferal proxy to estimate dysoxic bottom water oxygen concentrations, Santa Barbara Basin, US Pacific continental margin. *Journal of Foraminiferal Research* 27, 301–310.

- Bernhard, J.M., Goldstein, S.T., Bowser, S.S., 2010. An ectobiont-bearing foraminifera, *Bolivina pacifica*, that inhabits microoxic pore waters: cell-biological and paleoceanographic insight. *Environmental Microbiology* 12 (8), 2107–2119.
- Bijl, P.K., Houben, A.J.P., Schouten, S., Bohaty, S.M., Sluijs, A., Reichert, G.-J., Sinninghe Damsté, J.S., Brinkhuis, H., 2010. Transient middle Eocene atmospheric CO₂ and temperature variations. *Science* 330, 819–821.
- Bohaty, S.M., Zachos, J.C., 2003. A significant Southern Ocean warming event in the late middle Eocene. *Geology* 31, 1017–1020.
- Bohaty, S.M., Zachos, J.C., Florindo, F., Delaney, M.L., 2009. Coupled greenhouse warming and deep-sea acidification in the Middle Eocene. *Paleoceanography* 24 (PA2207). <http://dx.doi.org/10.1029/2008PA001676>.
- Boltovskoy, E., Scott, D.B., Mediolì, F.S., 1991. Morphological variations of benthic foraminiferal tests in response to changes in ecological parameters, a review. *Journal of Paleontology* 65, 175–185.
- Bosellini, A., 1989. Dynamics of Tethyan carbonate platform. In: Crevello, P.D., James, L.W., Sarg, J.F., Read, J.F. (Eds.), *Controls on Carbonate Platform and Basin Platform: Society for Sedimentary Geology (SEPM) Special Publication*, vol. 44, pp. 3–13.
- Bowen, G.J., Zachos, J.C., 2010. Rapid carbon sequestration at the termination of the Palaeocene–Eocene Thermal Maximum. *Nature Geoscience* 3, 866–869.
- Bradshaw, J.S., 1961. Laboratory experiments on the ecology of foraminifera. *Contributions from the Cushman Foundation of Foraminiferal Research*, 12 87–106.
- Braga, G., De Biase, R., Grünig, A., Proto Decima, F., 1975. Foraminiferi bentonici del Paleocene ed Eocene della sezione di Possagno. In: Bolli, H.M. (Ed.), *Monografia Micropaleontologica sul Paleocene e l'Eocene di Possagno: Provincia di Treviso, Italia: Schweizerische Palaeontologische Abhandlungen*, 97, pp. 87–199.
- Buzas, M.A., Culver, S.J., Jorissen, F.J., 1993. A statistical evaluation of the microhabitats of living (stained) infaunal benthic foraminifera. *Marine Micropaleontology* 29, 73–76.
- Cita, M.B., 1975. Stratigrafia della Sezione di Possagno. In: Bolli, H.M. (Ed.), *Monografia Micropaleontologica sul Paleocene e l'Eocene di Possagno: Provincia di Treviso, Italia: Schweizerische Palaeontologische Abhandlungen*, 97, pp. 9–33.
- Corliss, B.H., 1985. Microhabitats of Benthic Foraminifera within deep-sea sediments. *Nature* 314, 435–438.
- Corliss, B.H., Chen, C., 1988. Morphotype patterns of Norwegian Sea deep-sea benthic foraminifera and ecological implications. *Geology* 16, 716–719.
- Coxall, H.K., Wilson, P.A., Palike, H., Lear, C.H., Backman, J., 2005. Rapid stepwise onset of Antarctic glaciation and deeper calcite compensation in the Pacific Ocean. *Nature* 433 (7021), 53–57.
- Diester-Haass, L., Robert, C., Chamley, H., 1998. Paleoproductivity and climate variations during sapropel deposition in the eastern Mediterranean Sea. In: Robertson, A.H.F., Emeis, K.-C., Richter, C., Camerlenghi, A. (Eds.), *Proceedings of the Ocean Drilling Program, Scientific Results*, 160, pp. 227–248.
- Edgar, K.M., Wilson, P.A., Sexton, P.F., Suganuma, Y., 2007. No extreme bipolar glaciation during the main Eocene calcite compensation shift. *Nature* 448, 908–911.
- Edgar, K.M., Wilson, P.A., Sexton, P.F., Gibbs, S.J., Roberts, A.P., Norris, R.D., 2010. New biostratigraphic, magnetostratigraphic and isotopic insights into the Middle Eocene Climatic Optimum in low latitudes. *Palaeogeography, Palaeoclimatology, Palaeoecology* 297, 670–682.
- Fontanier, C., Jorissen, F.J., Licari, L., Alexandre, A., Anschutz, P., Carbonel, P., 2002. Live benthic foraminiferal faunas from the Bay of Biscay: faunal density, composition, and microhabitats. *Deep-Sea Research* 49, 751–785.
- Fontanier, C., Jorissen, F.J., Chaillou, G., Anschutz, P., Grémare, A., Griveaud, C., 2005. Live foraminiferal faunas from a 2800 m deep lower canyon station from the Bay of Biscay: faunal response to focusing of refractory organic matter. *Deep-Sea Research* 52, 1189–1227.
- Friedrich, O., 2009. Benthic foraminifera and their role to decipher paleoenvironment during mid-Cretaceous Oceanic Anoxic Events the “anoxic benthic foraminifera paradox”. *Revue de Micropaleontology* 177, 2–18.
- Friedrich, O., Nishi, H., Pross, J., Schmiedel, G., Hemleben, C., 2005. Millennial-to centennial scale interruptions of the Oceanic Anoxic Event 1b (early Albian, mid Cretaceous) inferred from benthic foraminiferal repopulation events. *Palaios* 20, 64–77.
- Galeotti, S., Krishnan, S., Pagani, M., Lanci, L., Gaudio, A., Zachos, J.C., Monechi, S., Morelli, G., Lourens, L., 2010. Orbital chronology of Early Eocene hyperthermals from the Contessa Road section, central Italy. *Earth and Planetary Science Letters* 290, 192–200.
- Giusberti, L., Coccioni, R., Sprovieri, M., Tateo, F., 2009. Perturbation at the sea floor during the Paleocene–Eocene Thermal Maximum: evidence from benthic foraminifera at Contessa Road, Italy. *Marine Micropaleontology* 70, 102–119.
- Gooday, A.J., 1996. Epifaunal and shallow infaunal foraminiferal communities at three abyssal NE Atlantic sites subject to differing phytodetritus input regimes. *Deep-Sea Research* 43, 1395–1421.
- Gooday, A.J., 2003. Benthic foraminifera (Protista) as tools in deepwater palaeoceanography: environmental influences on faunal characteristics. *Advances in Biology* 46, 1–90.
- Gooday, A.J., Rathburn, A.E., 1999. Temporal variability in living deep-sea benthic foraminifera. *Earth-Science Reviews* 46, 187–212.
- Green, M.A., Aller, R.C., Aller, J.Y., 1993. Carbonate dissolution and temporal abundances of Foraminifera in Long Island Sound sediments. *Limnology and Oceanography* 38 (2), 331–345.
- Grünig, A., 1984. Phenotypic variation in *Spiroplectamina*, *Uvigerina* and *Bolivina*. Benthos 1983. Second Symposium on Benthic Foraminifera (Pau, April 1983), pp. 249–255.
- Grünig, A., 1985. Systematical description of Eocene foraminifera of Possagno (Northern Italy), Sansoain (Northern Spain) and Biarritz (Aquitaine, France). *Memorie di Scienze Geologiche* 37, 251–302.
- Grünig, A., Herb, R., 1980. Paleoecology of late Eocene benthonic foraminifera from Possagno (Treviso-Northern Italy). *Cushman Foundation Special Publication* 18, 68–85.
- Hagn, H., 1956. Geologische und Paläontologische untersuchungen im Tertiär des Monte Brione und seiner umgebung (Gardasee, Ober-Italien). *Palaeontographica Abteilung A* 107, 67–210.
- Hammer, Ø., Harper, D.A.T., Ryan, P.D., 2001. PAST: Paleontological Statistics Software Package for Education and Data Analysis. *Palaeontologia Electronica* 4 (1) (9 pp., http://paleoelectronica.org/2001_1/past/issue1_01.htm).
- Herguera, J.C., Berger, W.H., 1991. Paleoproductivity from benthic foraminiferal abundance: glacial to postglacial changes in the west equatorial Pacific. *Geology* 19, 1173–1176.
- Hoenisch, B., Ridgwell, A., Schmidt, D.N., Thomas, E., Gibbs, S.J., Sluijs, A., Zeebe, R., Kump, L., Martindale, R.C., Greene, S.E., Kiessling, W., Ries, J., Zachos, J.C., Royer, D.L., Barker, S., Marchitto Jr., T.M., Moyer, R., Pelejero, C., Ziveri, P., Foster, G.L., Williams, B., 2012. The geological record of ocean acidification. *Science* 335, 1058–1063.
- Jones, R.W., Charnock, M.A., 1985. “Morphogroups” of agglutinated foraminifera. Their life positions and feeding habits and potential applicability in (paleo)ecological studies. *Revue de Paléobiologie* 4, 311–320.
- Jorissen, F.J., 1999. Benthic foraminiferal successions across late Quaternary Mediterranean sapropels. In: Rohling, E.J. (Ed.), *Fifth decade of Mediterranean paleoclimate and sapropel studies: Marine Geology*, 153, pp. 91–101.
- Jorissen, F.J., De Stigter, H.C., Widmark, J.G.V., 1995. A conceptual model explaining benthic foraminiferal microhabitats. *Marine Micropaleontology* 26, 3–15.
- Jorissen, F.J., Fontanier, C., Thomas, E., 2007. Paleogeographical proxies based on deep-sea benthic foraminiferal assemblage characteristics. In: Hillaire-Marcel, C., de Vernal, A. (Eds.), *Developments in Marine Geology: Proxies in Late Cenozoic Paleoclimatology*, vol. 1. Elsevier, Amsterdam, pp. 264–325.
- Jovane, L., Florindo, F., Coccioni, R., Dinare's-Turell, J., Marsili, A., Monechi, S., Roberts, A.P., Sprovieri, M., 2007. The middle Eocene climatic optimum event in the Contessa Highway section, Umbrian Apennines, Italy. *Geological Society of America Bulletin* 119, 413–427. <http://dx.doi.org/10.1130/B25917.1>.
- Kaminski, M.A., Gradstein, F.M., 2005. Atlas of Paleogene Cosmopolitan Deep-water Agglutinated Foraminifera. *Gryzbowski Foundation Special Publication* 10. 547 (+ pp. vii).
- Katz, M., Thunell, R., 1984. Benthic foraminiferal biofacies associated with middle Miocene to early Pliocene oxygen-deficient conditions in the eastern Mediterranean. *Journal of Foraminiferal Research* 14 (3), 187–202.
- Katz, M.E., Miller, K.G., Wright, J.D., Wade, B.S., Browning, J.V., Cramer, B.S., Rosenthal, Y., 2008. Stepwise transition from the Eocene greenhouse to the Oligocene icehouse. *Nature Geoscience* 1, 329–334.
- Kitazato, H., Ohga, T., 1995. Seasonal changes in deep-sea benthic foraminiferal populations: results of long-term observations at Sagami Bay, Japan. In: Sakai, H., Nozaki, Y. (Eds.), *Biogeochemical Processes and Ocean Flux Studies in the Western Pacific*. Terra Scientific, Tokyo, pp. 331–342.
- Koutsoukos, E.A.M., Leary, P.M., Hart, M.B., 1990. Latest Cenomanian–earliest Turonian low-oxygen tolerant benthonic foraminifera: a case study from the Sergipe Basin (NE Brazil) and the western Anglo-Paris Basin (southern England). *Palaeogeography, Palaeoclimatology, Palaeoecology* 77, 145–177.
- Kuhnt, W., Wiedmann, J., 1995. Cenomanian–Turonian source rocks: paleobiogeographic and paleoenvironmental aspects. In: Huc, A.Y. (Ed.), *Paleogeography, Paleoclimate and Source Rocks: American Association of Petroleum Geologists, Studies in Geology*, pp. 213–232.
- Lear, C.H., Bailey, T.R., Pearson, P.N., Coxall, H.K., Rosenthal, Y., 2008. Cooling and ice growth across the Eocene–Oligocene transition. *Geology* 36 (3), 251–254.
- Levin, L.A., Etter, R.J., Rex, M.A., Gooday, A.J., Smith, C.R., Pineda, J., Stuart, C.T., Hessler, R.R., Pawson, D., 2001. Environmental influences on regional deep-sea species diversity. *Annual Review of Ecology and Systematics* 132, 51–93.
- Loubere, P., 1991. Deep sea benthic foraminiferal assemblage response to a surface ocean productivity gradient: a test. *Paleoceanography* 6, 193–204.
- Loubere, P., 1996. The surface ocean productivity and bottom water oxygen signals in deep water benthic foraminiferal assemblages. *Marine Micropaleontology* 28, 247–261.
- Loubere, P., 1997. Benthic foraminiferal assemblage formation, organic carbon flux and oxygen concentrations on the outer continental shelf and slope. *Journal of Foraminiferal Research* 27, 93–100.
- Loubere, P., Fariduddin, M., 1999a. Quantitative estimation of global patterns of surface ocean biological productivity and its seasonal variation on timescales from centuries to millennia. *Global Biogeochemical Cycles* 13, 115–133. <http://dx.doi.org/10.1029/1998GB900001>.
- Loubere, P., Fariduddin, M., 1999b. Benthic foraminifera and the flux of organic carbon to the seabed. In: Sen Gupta, B.K. (Ed.), *Modern Foraminifera*. Kluwer, Dordrecht, pp. 181–199.
- Luciani, V., Giusberti, L., Agnini, C., Fornaciari, E., Rio, D., Spofforth, D.J.A., Pälke, H., 2010. Ecological and evolutionary response of Tethyan planktonic foraminifera to the middle Eocene climatic optimum (MECO) from the Alano section (NE Italy). *Palaeogeography, Palaeoclimatology, Palaeoecology* 292, 82–95. <http://dx.doi.org/10.1016/j.palaeo.2010.03.029>.
- Lunt, D., Ridgwell, A., Sluijs, A., Zachos, J., Hunter, S., Haywood, A., 2011. A model for orbital pacing of methane hydrate destabilization during the Palaeogene. *Nature Geoscience* 4, 775–778.
- Lutze, G.F., Coulbourn, W.T., 1984. Recent benthic foraminifera from the continental margin of Northwest Africa; community structure and distribution. *Marine Micro-paleontology* 8, 361–401.
- Martini, E., 1971. Standard Tertiary and Quaternary calcareous nannoplankton zonation. In: Farinacci, A. (Ed.), *Proceedings of the 2nd Planktonic Conference*, 2, Ed. Tecnoscienza, Roma, pp. 739–785.
- McInerney, F.A., Wing, S.L., 2011. The Paleocene–Eocene thermal maximum: a perturbation of carbon cycle, climate, and biosphere with implications for the future. *Annual Review of Earth and Planetary Sciences* 39, 489–516. <http://dx.doi.org/10.1146/annurev-earth-040610-133431>.

- Miller, K.G., Fairbanks, R.G., Mountain, G.S., 1987. Tertiary oxygen isotope synthesis, sea level history, and continental margin erosion. *Paleoceanography* 2 (1), 1–19.
- Miller, K.G., Wright, J.D., Browning, J.V., 2005. Visions of ice sheets in a greenhouse world. *Marine Geology* 217, 215–231.
- Morigi, C., 2009. Benthic environmental changes in the Eastern Mediterranean Sea during sapropel S5 deposition. *Palaeogeography, Palaeoclimatology, Palaeoecology* 273, 258–271.
- Morigi, C., Jorissen, F.J., Gervais, A., Guichard, S., Borsetti, A.M., 2001. Benthic foraminiferal faunas in surface sediments off NW Africa: relationship with organic flux to the ocean floor. *Journal of Foraminiferal Research* 31, 350–368.
- Murray, J.W., 2001. The niche of benthic foraminifera, critical thresholds and proxies. *Marine Micropaleontology* 41, 1–7.
- Murray, J.W., 2006. *Ecology and Applications of Benthic Foraminifera*. Cambridge University Press 426 (+ pp. xi).
- Murray, J.W., 2013. Living benthic foraminifera: biogeographic distributions and the significance of rare morphospecies. *Journal of Micropaleontology* 32, 1–58.
- Okada, H., Bukry, D., 1980. Supplementary modification and introduction of code numbers to the low-latitude coccolith biostratigraphic zonation (Bukry, 1973; 1975). *Marine Micropaleontology* 5, 321–325.
- Ortiz, S., Thomas, E., 2006. Lower-middle Eocene benthic foraminifera from the Fortuna Section (Betic Cordillera, south-eastern Spain). *Micropaleontology* 52 (2), 97–150.
- Ortiz, S., Gonzalvo, C., Molina, E., Rodriguez-Tovar, F.J., Uchman, A., Vandenbergh, N., Zeelmaekers, E., 2008. Palaeoenvironmental turnover across the Ypresian–Lutetian transition at the Agost section, Southwestern Spain: In search of a marker event to define the Stratotype for the base of the Lutetian Stage. *Marine Micropaleontology* 69, 297–313.
- Pagani, M., Zachos, J.C., Freeman, K.H., Tipler, B., Bohaty, S., 2005. Marked decline in atmospheric carbon dioxide concentrations during the Paleogene. *Science* 309, 600–603.
- Parisi, G., Coccioni, R., 1988. Deep-water benthic foraminifera at the Eocene–Oligocene boundary in the Massignano section (Ancona, Italy). *International Subcommission on Paleogene Stratigraphy, E/O Meeting (Ancona, October 1987) Special Publication II 3*, pp. 97–109.
- Phleger, F.B., Soutar, A., 1973. Production of benthic foraminifera in three east Pacific oxygen minima. *Micropaleontology* 19, 110–115.
- Pierrehumbert, R.T., 2002. The hydrologic cycle in deep-time climate problems. *Nature* 419, 191–198.
- Schmiedl, G., Mitschele, A., Beck, S., Emeis, K.C., Hemleben, C., Schulz, H., Sperling, M., Weldeab, S., 2003. Benthic foraminiferal record of ecosystem variability in the eastern Mediterranean Sea during times of sapropel S5 and S6 deposition. *Palaeogeography, Palaeoclimatology, Palaeoecology* 190, 139–164.
- Schroeder, C.J., Scott, D.B., Medioli, F.S., 1987. Can smaller benthic foraminifera be ignored in paleoenvironmental analyses? *Journal of Foraminiferal Research* 17, 101–105.
- Sen Gupta, B.K., Machain-Castillo, M.L., 1993. Benthic foraminifera in oxygen-poor habitats. *Marine Micropaleontology* 20, 3–4.
- Sexton, P.F., Wilson, P.A., Norris, R.D., 2006. Testing the Cenozoic multisite composite $\delta^{18}\text{O}$ and $\delta^{13}\text{C}$ curves: new monospecific Eocene records from a single locality, Demerara Rise (Ocean Drilling Program Leg 207). *Paleoceanography* 21 (2), PA2019.
- Silva, K.A., Corliss, B.H., Rathburn, A.E., Thunell, R.C., 1996. Seasonality of living benthic foraminifera from the San Pedro basin, California borderland. *Journal of Foraminiferal Research* 26, 71–93.
- Sluijs, A., Bowen, G.J., Brinkhuis, H., Lourens, L.J., Thomas, E., 2007. The Paleocene–Eocene Thermal Maximum super greenhouse: biotic and geochemical signatures, age models and mechanisms of global change. In: Williams, M., Haywood, A.M., Gregory, F.J., Schmidt, D.N. (Eds.), *Deep-time Perspectives on Climate Change: Marrying the Signal from Computer Models and Biological Proxies: The Micropaleontological Society, Special Publication*, pp. 323–349.
- Spofforth, D.J.A., Agnini, C., Pälke, H., Rio, D., Fornaciari, E., Giusberti, L., Luciani, V., Lanci, L., Muttoni, G., 2010. Organic carbon burial following the Middle Eocene Climatic Optimum (MECO) in the central-western Tethys. *Paleoceanography* 25, PA3210.
- Sprong, J., Kouwenhoven, T.J., Bornemann, A., Schulte, P., Stassen, P., Steurbaut, E., Youssef, M., Speijer, R.P., 2012. Characterization of the Latest Danian Event by means of benthic foraminiferal assemblages along a depth transect at the southern Tethyan margin (Nile Basin, Egypt). *Marine Micropaleontology* 86–87, 15–31.
- Stap, L., Lourens, L.J., Thomas, E., Sluijs, A., Bohaty, S., Zachos, J.C., 2010. High-resolution deep-sea carbon and oxygen isotope records of Eocene Thermal Maximum 2 and H2. *Geology* 38, 208–210.
- Stickley, C.E., St John, K., Koc, N., Jordan, R.W., Passchier, S., Pearce, R.B., Learns, L.E., 2009. Evidence for middle Eocene Arctic sea ice from diatoms and ice-rafted debris. *Nature* 460, 376–379.
- Thomas, E., 1985. Late Eocene to Holocene deep-sea benthic foraminifera from the central equatorial Pacific Ocean. In: Mayer, L., et al., eds., *Initial Reports of the Deep Sea Drilling Project*, Washington D.C., U.S. Government Printing Office, v. 85, pp. 141–165.
- Thomas, E., 2003. Extinction and food at the sea floor: a high resolution benthic foraminiferal record across the Initial Eocene Thermal Maximum, Southern Ocean Site 690. In: Wing, S., Gingerich, P., Schmitz, B., Thomas, E. (Eds.), *Causes and Consequences of Globally Warm Climates of the Paleogene: The Geological Society of America Special Paper*, vol. 369, pp. 319–332.
- Thomas, E., Booth, L., Maslin, M., Shackleton, N.J., 1995. Northeastern Atlantic benthic foraminifera during the last 45,000 years: changes in productivity seen from the bottom up. *Paleoceanography* 10, 545–562. <http://dx.doi.org/10.1029/94PA03056>.
- Toffanin, F., Agnini, C., Fornaciari, E., Rio, D., Giusberti, L., Luciani, V., Spofforth, D.J.A., Pälke, H., 2011. Changes in calcareous nannofossil assemblages during the Middle Eocene Climatic Optimum: clues from the central-western Tethys (Alano section, NE Italy). *Marine Micropaleontology* 81, 22–31.
- Trevisani, E., 1997. *Stratigrafia sequenziale e paleogeografia del margine orientale del Lessini Shelf durante l'Eocene superiore (Prealpi Venete, provincie di Vicenza e Treviso)*. Studi Trentini di Scienze Naturali. *Acta Geologica* 71 (1994), 145–168.
- Tripati, A., Backman, J., Elderfield, H., Ferretti, P., 2005. Eocene bipolar glaciation associated with global carbon cycle changes. *Nature* 436, 341–346.
- Valiela, I., 1984. *Marine Ecological Process*. Springer, New York (546 pp.).
- Van Morkhoven, F.P.C.M., Berggren, W.A., Edwards, A.S., 1986. Cenozoic Cosmopolitan deep-sea benthic foraminifera. *Bulletin des Centres de Recherches Exploration-Production Elf-Aquitane, Mémoire* 11, 11–421.
- Van der Zwaan, G.J., Duijnste, I.A.P., Den Dulk, M., Ernst, S.R., Kouwenhoven, N.T., 1999. Benthic foraminifera: proxies or problems? A review of paleoecological concepts. *Earth Science Reviews* 46, 213–236.
- Winterer, E.L., Bosellini, A., 1981. Subsidence and sedimentation on Jurassic passive continental margin, Southern Alps, Italy. *American Association of Petroleum Geologists Bulletin* 65, 394–421.
- Witkowski, J., Bohaty, S.M., McCartney, K., Harwood, D.M., 2012. Enhanced siliceous plankton productivity in response to middle Eocene warming at Southern Ocean ODP Sites 748 and 749. *Palaeogeography, Palaeoclimatology, Palaeoecology* 326–328, 78–94.
- Zachos, J.C., Quinn, T.M., Salamy, K.A., 1996. High resolution (104 years) deep sea foraminiferal stable isotope records of the Eocene–Oligocene climate transition. *Paleoceanography* 11 (3), 251–266.
- Zachos, J.C., Pagani, M., Sloan, L.C., Thomas, E., Billups, K., 2001. Trends, rhythms, and aberrations in global climate 65 Ma to present. *Science* 292, 686–693.
- Zachos, J.C., Röhl, U., Schellenberg, S.A., Sluijs, A., Hodell, D.A., Kelly, D.C., Thomas, E., Nicolo, M., Raffi, I., Lourens, L.J., McCarren, H., Kroon, D., 2005. Rapid acidification of the ocean during the Paleocene–Eocene Thermal Maximum. *Science* 308, 1611–1615.
- Zachos, J.C., Dickens, G.R., Zeebe, R.E., 2008. An early Cenozoic perspective on greenhouse warming and carbon-cycle dynamics. *Nature* 451, 279–283. <http://dx.doi.org/10.1038/nature06588>.
- Zachos, J.C., McCarren, H.K., Murphy, B., Röhl, U., Westerhold, T., 2010. Tempo and scale of late Paleocene and early Eocene carbon isotope cycles: implications for the origin of hyperthermals. *Earth and Planetary Science Letters* 299 (1–2), 242–249.